

EFFECTS OF TRISILANOL POLYHEDRAL SILSESQUIOXANES ADDITIONS ON
ALUMINUM ALLOYS:
SURFACE AND ELECTROCHEMICAL CHARACTERISTICS

By

Yuxiang Zhong

A THESIS

Submitted to
Michigan State University
in partial fulfillment of the requirements
for the degree of

Materials Science and Engineering—Master of Science

2019

ABSTRACT

EFFECTS OF TRISILANOL POLYHEDRAL SILSESQUIOXANES ADDITIONS ON ALUMINUM ALLOYS: SURFACE AND ELECTROCHEMICAL CHARACTERISTICS

By

Yuxiang Zhong

In the automotive industry, aluminum alloys are of particular interests in providing the fuel economy needed to meet the required Corporate Average Fuel Economy (CAFE) standards. Current commercial cast aluminum alloys use Strontium (Sr) to modify the eutectic silicon morphology leading to improve ductility. However, the fading of Sr addition effect at the molten temperature remains as a major concern. Recently, it was demonstrated that the addition of nanostructured silanol based on polyhedral silsesquioxanes to cast aluminum alloys provided the refinement of eutectic silicon morphology without fading when held at molten temperature up to 96 hours. In addition, using master ingots containing nanostructured silanols, large-scale commercial alloys have been successfully modified.

In this work, aluminum coated with nanostructured silanol of different chemical moieties were investigated. The contact angle measurement and powder sedimentation experiments have shown the increase in the hydrophobicity with nanostructured silanol coating. In addition, durability of the coating was also examined. Secondly, we investigated the electrochemical behavior of several casted aluminum alloys. The open circuit potential measurement and potentiodynamic polarization measurement show that the microstructure refinement with Sr or TSP will not affect the corrosion behavior on the hypo-eutectic Al-Si alloys but will reduce the anodic current density of the eutectic Al-Si alloys.

ACKNOWLEDGEMENTS

First, I am extremely grateful to Dr. Andre Lee for being my academic advisor, who gives me this great opportunity to continue my graduate study in Michigan State University. His knowledge, creativeness and patience help me tackle a lot of difficulties in my research study. I would also like to thank my committee members – Dr. Shiwang Cheng and Dr. Wei Lai – for their guidance and kindness. Dr. Cheng always gives me some intelligent suggestions and corrects my mistakes during my research study. Dr. Lai generously provides me access to use their equipment and lab facility to do experiments of my research.

Second, a lot appreciate to my lab mates for their helps and kindness, especially for Dr. Yang Lu, Dr. Yuelin Wu, Dr. David Vogelsang and future Dr. Tyler Johnson. Dr. Yang Lu as my first mentor in this lab, taught me to use different equipment, showed me different laboratories, guided me in my research study. He and his wife Dr. Chun Liu often invited me to their home to visit. It was such great days before they leave MSU. Dr. Yuelin Wu as my second mentors in our lab helped me a lot in electrochemical study. His brilliant point of view for things always inspire me. Dr. David Vogelsang and Mr. Tyler Johnson often tell me some interesting thing and their fantastic characteristic make my graduate study much fun. I appreciate all of them to play such important roles in my graduate student life. I sincerely wish every one of them have a bright future.

At last, I want to thank my father Nianchao Zhong and mother Jingwen Ding, who give me all their love, and both emotionally and financially support to let me study in the United States. Furthermore, I would like to thank my girlfriend Xue Jiang, who is always by my side at the most difficult times, and makes my life much more wonderful in MSU.

TABLE OF CONTENTS

LIST OF FIGURES	v
CHAPTER 1 INTRODUCTION AND RESEARCH STRATEGIES	1
CHAPTER 2 PERFORMANCE OF TRISILANOL POSS COATING AND MODIFIED ALLOYS	5
2.1 Introduction	5
2.2 Materials and Methods	5
2.2.1 Materials	5
2.2.2 Aluminum 7075 T6/Copper Plates Preparation.....	6
2.2.3 Contact Angle Measurements.....	6
2.2.4 Aluminum/Copper Sample Powder Preparation	7
2.2.5 Hydrophobicity Test of Sample Powders	7
2.2.6 Corrosion Tests of Copper Powders	7
2.2.7 Binary Aluminum Alloy and Aural 2 Sample Plates Preparation	8
2.2.8 Droplets Contact Area Measurements	8
2.3 Results and Discussions	8
2.3.1 Effect of Oxidation Layer on Aluminum Surface	8
2.3.2 Aluminum Substrates	9
2.3.3 Copper Substrates	14
2.3.4 Modified Al-Alloy Substrates	21
2.4 Conclusions	24
CHAPTER 3 EFFECT OF MICROSTRUCTURE ON POLARIZATION BEHAVIOR OF AL-SI BASED CASTING ALLOYS	26
3.1 Introduction	26
3.2 Materials and Methods	26
3.2.1 Sample preparation	26
3.2.2 Electrochemical Characterization.....	27
3.2.3 Electrode Preparation	27
3.2.4 Electrolyte Preparation	27
3.2.5 Open Circuit Potential Measurement	28
3.2.6 Potentiodynamic Polarization Measurement	29
3.3 Results and Discussions	30
3.4 Conclusions	38
CHAPTER 4 SUMMARY AND FUTURE WORK	40
4.1 Summary	40
4.2 Future Work	42
BIBLIOGRAPHY	44

LIST OF FIGURES

Figure 1. Schematic of structure of TSP.....	1
Figure 2. Optical Micrographs of the As-cast Al-7.5Si Alloy: (a) Al-7.5Si Base, (b) Al-7.5Si with Sr, and (c) Al-7.5Si with TSP under 5x,20x, and 100x magnification. [2]	3
Figure 3. Optical Micrographs of the As-cast Al-7.5Si Alloy: (a) Aural™ 2 without Sr, (b) Aural™ 2 with TSP, (c) Aural™ 2 with Sr, (d) W319 base, and (e) W319 with TSP under 5x,20x, and 100x magnification. [2].....	4
Figure 4. Side-view images of the water droplet on polished and HCl-cleaned Al plate exposed to air over 0 min,1 min, 2 min, 4 min, 8 min, 16 min, 30min, 60 min, and 6 hours.....	9
Figure 5. Images of 5mg Al powders soaked in 30 mL deionized water: (a) untreated Al, (b) Ph-TSP treated Al, (c) Et-TSP treated Al, and (d) iBu-TSP treated Al.	10
Figure 6. 45°-view images of Al sheet with two water drops on the top: (a) untreated Al, (b) Ph-TSP treated Al, (c) Et-TSP treated Al, and (d) iBu-TSP treated Al.....	11
Figure 7. Side-view images of Al sheet with three water drops on the top: (a) untreated Al, (b) Ph-TSP treated Al, (c) Et-TSP treated Al, and (d) iBu-TSP treated Al.....	11
Figure 8. Contact angle measurements for untreated Al, Ph-TSP treated Al, Et-TSP treated Al, and iBu-TSP treated Al.....	12
Figure 9. Contact angle measurements for Ph-TSP treated Al plate (a) soaked in 2% Ph-treated Ethanol (b) physically wiped (c) re-soaked in pure Ethanol for 5 days.....	13
Figure 10. Contact angle measurements for Et-TSP treated Al plate (a) soaked in 2% Et-treated Ethanol (b) physically wiped (c) re-soaked in pure Ethanol for 5 days.....	13
Figure 11. Contact angle measurements for iBu-TSP treated Al plate (a) soaked in 2% iBu-treated Ethanol (b) physically wiped (c) re-soaked in pure Ethanol for 5 days.....	13

Figure 12. Images of 3g Cu powders soaked in 30 mL deionized water: (a) untreated Cu, (b) iBu-TSP treated Cu, and (c) Ph-TSP treated Cu.....	15
Figure 13. 45°-view imagines of Cu sheet with two water drops on the top: (a) untreated Cu, (b) Ph-TSP treated Cu, (c) Et-TSP treated Cu, and (d) iBu-TSP treated Cu.....	16
Figure 14. Side-view imagines of Cu sheet with three water drops on the top: (a) untreated Cu, (b) Ph-TSP treated Cu, (c) Et-TSP treated Cu, and (d) iBu-TSP treated Cu.	16
Figure 15. Contact angle measure for untreated Cu, Ph-TSP treated Cu, Et-TSP treated Cu, and iBu-TSP treated Cu.	17
Figure 16. Images of 3g as received, iBu-TSP treated, and Ph-TSP treated Cu powders soaked in 30mL 3.5 wt% NaCl water up to 60 hours.	19
Figure 17. Images of 3g as received, iBu-TSP treated, and Ph-TSP treated Cu powders soaked in 30mL 3.5 wt% NaCl water from 4 days up to 16 days.	20
Figure 18. Side-view for (a) Al-7.5Si-untreated, (b) Al-7.5Si-TSP, and (c) Al-7.5Si-Sr. Top-view for (d) Al-7.5Si-untreated, (e) Al-7.5Si-TSP, and (f) Al-7.5Si-Sr.....	21
Figure 19. Side-view for (a) Aural 2 without Sr, (b) Aural 2 with TSP, and (c) Aural 2 with Sr. Top-view for (d) Aural 2 without Sr, (e) Aural 2 with TSP, and (f) Aural 2 with Sr.....	22
Figure 20. Contact angles measurements for Al-7.5Si alloy (top left) and Aural 2 alloy (top right); contact areas measurements for Al-7.5Si alloy (bottom left) and Aural 2 alloy (bottom right).	22
Figure 21. SEM Micrographs of the Deep-etched Aural™ 2 Alloys: (a) Aural™ 2 Base, (b) Aural™ 2 with TSP, and (c) Aural™ 2 with Sr. [2].....	23
Figure 22. Schematic illustration of sample encapsulation.	27
Figure 23. Two-electrode configuration for the Open Circuit Potential Measurement.	29
Figure 24. Three-electrode configuration for the potentiodynamic polarization measurements..	30

Figure 25. Polarization curves of Al-7.5Si Base, Aural2-Control, and W319-Control in an electrolyte solution containing 1wt% NaCl.	31
Figure 26. (a) Corrosion current density and (b) open circuit potential measurement of Al-7.5Si Base, Aural2-Control, and W319-Control.	32
Figure 27. Polarization curves of Al-7.5Si Base, Al-7.5Si-TSP, and Al-7.5Si-Sr in an electrolyte solution containing 1wt% NaCl.	33
Figure 28. Corrosion current density and open circuit potential measurement of Al-7.5Si Base, Al-7.5Si-TSP, and Al-7.5Si-Sr.	33
Figure 29. Polarization curves of Al-7.5Si, Al-7.5Si-0.5TSP, and Al-7.5Si-1TSP in electrolyte solution containing 1wt% NaCl.	34
Figure 30. Corrosion current density and open circuit potential measurement of Al-7.5Si, Al-7.5Si-0.5TSP, and Al-7.5Si-1TSP.	34
Figure 31. Polarization curves of W319-Control, and W319-TSP in an electrolyte solution containing 1wt% NaCl.	36
Figure 32. Corrosion current density and open circuit potential measurement of W319-Control, and W319-TSP.	36
Figure 33. Polarization curves of Aural2-Control, Aural2-TSP, and Aural2-Sr in an electrolyte solution containing 1wt% NaCl.	37
Figure 34. Corrosion current density and open circuit potential measurement of Aural2-Control, Aural2-TSP, and Aural2-Sr.	38

CHAPTER 1 INTRODUCTION AND RESEARCH STRATEGIES

The growth trend of using lightweight materials to replace conventional steel and cast irons in vehicles to improve the fuel economy and emissions attracts interests in the automotive industry. Although steel alloys are still the preferred materials by many automakers, the use of lightweight materials have significantly increased. The aluminum alloys are considered to be the cost-effective alternative lightweighting materials in replacing steel alloys. [1] The conventional aluminum-silicon (Al-Si) based casting alloys have high strength, but the ductility is limited due to their sensitivity to the crack initiation and propagation caused by the irregular eutectic silicon microconstituent in the as-cast condition. Modification of eutectic Si morphology by Strontium (Sr) has been the most common approach used in the commercially available high ductility casted aluminum alloys, but the oxidation of Sr at the casting temperature leading to the fading of Sr addition effect is a major concern. [2]

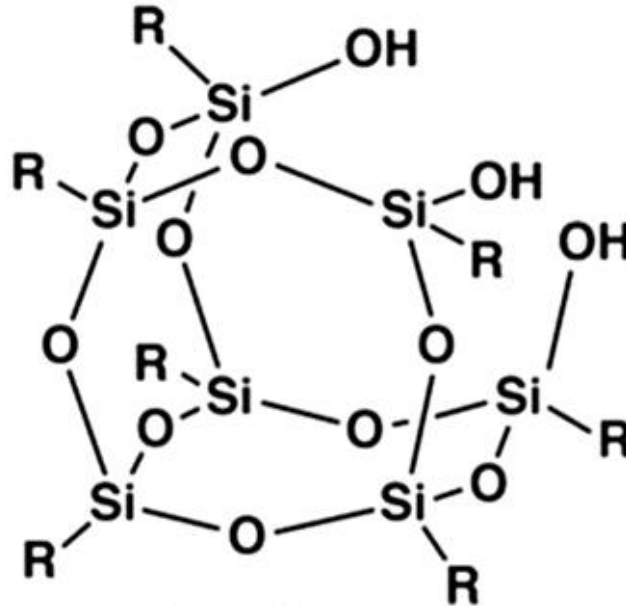


Figure 1. Schematic of structure of TSP.

Polyhedral oligomeric silsesquioxanes (POSS) molecules have cage-like structures with a general chemical structure of $R(SiO_{1.5})_n$ ($n=8, 10$ or 12) where R is organic moiety. [3] TriSilanol

Polyhedral Silsesquioxanes (TSP) as a class of POSS molecule having three reactive silanol groups at the vertex of the cube-like T₈-POSS as show in Figure 1. There are also examples in using functionalized POSS as the coating materials to improve material properties such as mechanical performance [4], fire retardants [5][6], hydrophobicity [7], biocompatibility [8], [9] and corrosion inhibition [10]–[12].

Recent studies have shown that TSP can be used as an aluminum modifier by dip coating process. They discovered that by dip-coating approach, TSP refined the microstructures of both primary Al and eutectic microconstituents of Al-12Si ingots. [2] Ductility was improved from 3% to 18% after TSP treatment. The bonds between TSP and Al can slow down the segregation of Al from the melting of Al-Si during the eutectic reaction, which leads to the refinement of the Al-Si eutectic microconstituents. With the support evidence of the laboratory-scale results, a new optimized TSP master with the composition consist of 6% TSP in an Al-12Si alloy was produced. After that, a 10% Al-12Si-6TSP master was applied to Al-Si binary alloys the commercial alloys at the 100 lbs. scale. The results showed that there is a 50% improvement in ductility over the Al-7.5Si base alloy, and the strength of alloys is not reduced. As Figure 2 shown, the addition of TSP successfully refined the microstructure of primary Al and eutectic microconstituents of the Al-7.5Si alloy. Only a small amount of Si fade was observed under 720 °C for up to 192 hours.

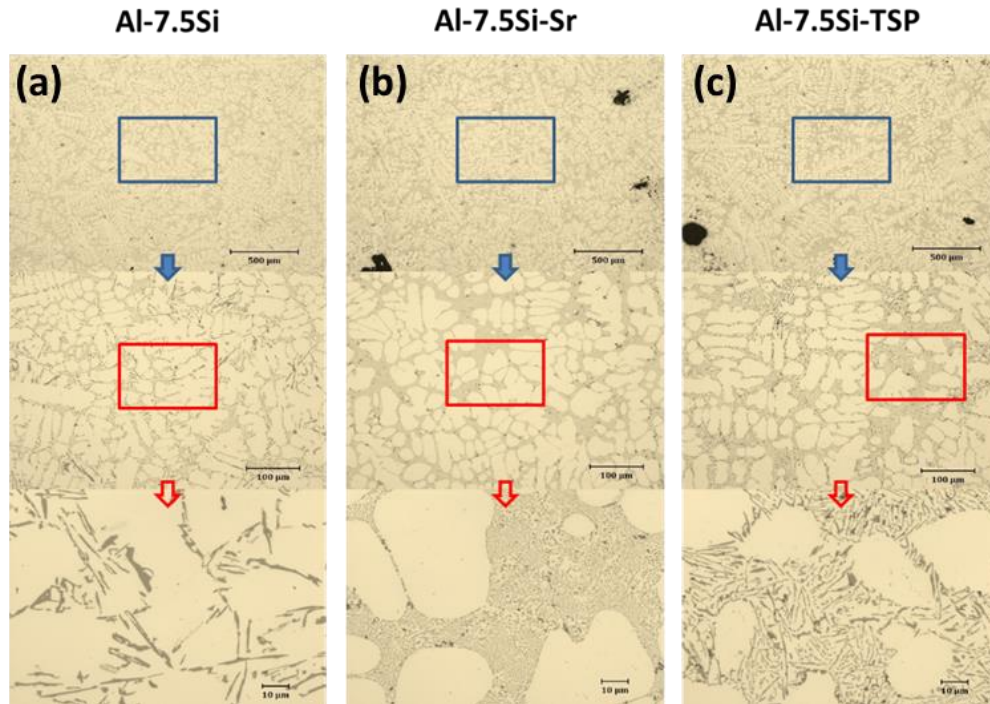


Figure 2. Optical Micrographs of the As-cast Al-7.5Si Alloy: (a) Al-7.5Si Base, (b) Al-7.5Si with Sr, and (c) Al-7.5Si with TSP under 5x,20x, and 100x magnification. [2]

For the commercial alloys such as AuralTM 2 and W319 base alloys, TSP not only reduced the shrinkage of the casting during the solidification, it also refined the Si in the Al-Si eutectic microconstituent as well as the Al secondary dendrite arm spacing as Figure 3 shown. The modification by TSP had a 100% improvement in ductility while maintaining the strength of alloys. [2]

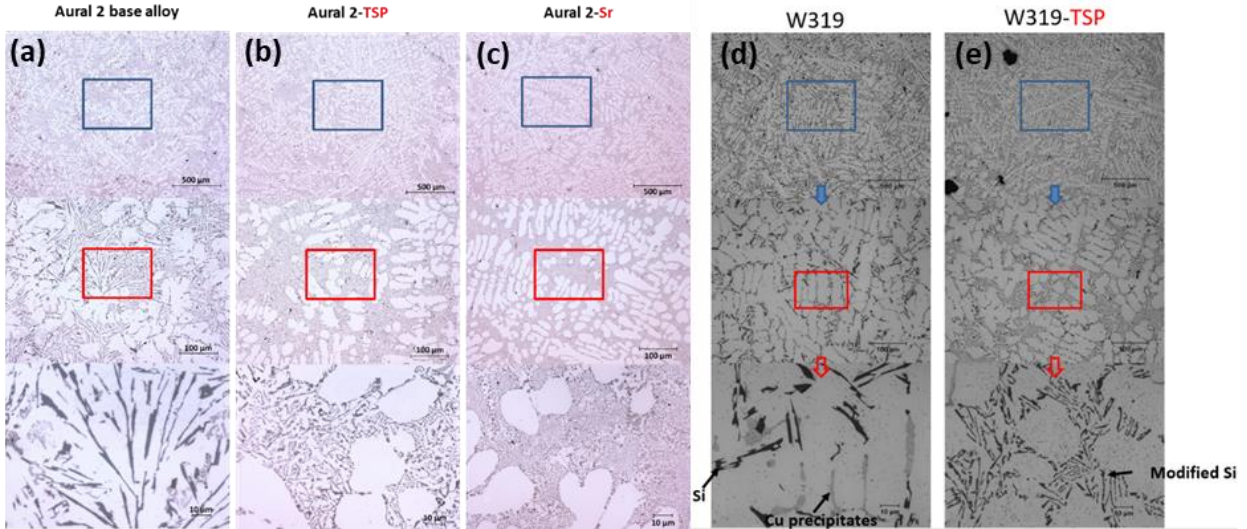


Figure 3. Optical Micrographs of the As-cast Al-7.5Si Alloy: (a) AuralTM 2 without Sr, (b) AuralTM 2 with TSP, (c) AuralTM 2 with Sr, (d) W319 base, and (e) W319 with TSP under 5x, 20x, and 100x magnification. [2]

To further investigate the performance of the TSP, it will be interesting to compare the results for both using TSP as coating material of aluminum alloys and using TSP as an aluminum modifier. Furthermore, studying the electrochemical behavior of Al-Si as-casted alloys after the refinement of microstructure by TSP addition will be a useful topic to determine the corrosion resistance of the materials.

In this thesis, we focused on two main topics which are (1) coating performance of TSP and (2) electrochemical behavior of TSP modified alloys. In Chapter 2, we used contact angle measurement and powder sedimentation experiments to investigate the coating performance on various aluminum alloys with different TSP surface treatment as well as the TSP modified materials. We have done the comparison group for TSP coating on Copper as well, especially for giving a more obvious performance during the powder sedimentation experiment. In Chapter 3, to study the electrochemistry behavior effect after TSP modification, the open circuit potential measurement and potentiodynamic polarization measurement were carried out for different aluminum alloys.

CHAPTER 2 PERFORMANCE OF TRISILANOL POSS COATING AND MODIFIED ALLOYS

2.1 Introduction

This chapter talks about the performance of TriSilanol POSS coating and performance of the modified alloys. We have used the contact angle measurements, soaking of metal powders and scanning electron microscopy (SEM) images to show the performance of coating or modification. Initially, we carried out the contact angle comparison for polished and cleaned aluminum 7075 T6 to investigate the influence of the oxidation layer. After that, the soaking experiment of powder aluminum and copper and contact measurement for aluminum and copper plates were done to compare the differences of several types of TSP coating. Due to the color of aluminum changes after rusting cannot be distinguished, while the bluish color of copper oxide is notable from the reddish color of copper, the rusting experiment of copper was carried out to show how the TSP coating benefits the material from being rusted. For the modified aluminum alloy, the contact angle measurement and SEM images of microstructures were used to show the differences among the Aural 2 aluminum without Sr, TSP-modified Aural 2 aluminum and Sr-modified Aural 2 aluminum.

2.2 Materials and Methods

2.2.1 Materials

Trisilanoethyl polyhedral oligomeric silsesquioxane (Et-TSP), Trisilanolisobutyl polyhedral oligomeric silsesquioxane (iBu-TSP), and Trisilanolphenyl polyhedral oligomeric silsesquioxane (Ph-TSP) were obtained from Hybrid Plastics, Inc. (Hattiesburg, MS). Powders of 30 μm 99.9% aluminum and 50 μm 99.5% copper were purchased from Alfa Aesar (Tewksbury, MA). The 50 μm A4047 powder with the nearly eutectic composition (nominal wt. %) of Al-12Si was manufactured by Johnson Manufacturing (Princeton, IA). Aluminum 7075 T6 plate and

copper plate were purchased from Comet Metals (Solon, OH). Two types of casted aluminum alloy were used in this study, Al-7.5Si binary alloy and Aural 2 alloy (Al-11%Si-0.3%Mg-0.5%Mn-0.2%Fe). Each group is comprised of an unmodified control sample, a TSP modified sample and a Sr modified sample. All the casted aluminum alloy ingots were produced in our laboratory as described in detail. [2] Chemicals used in this study are 200 Proof Pure Ethanol (Decon Labs, Inc.) and 36.46% Hydrochloric acid (Avantor Performance Materials, LLC).

2.2.2 Aluminum 7075 T6/Copper Plates Preparation

Plates of 40 mm × 10 mm × 2.5 mm were cut by metal cut-off machine (Struers Inc.) from the aluminum 7075 T6 ingot and were well-polished that no scratch can be seen on the surface. The plate samples were immersed in 5% HCl solution for 3 minutes at room temperature followed by DI water and pure Ethanol washing. Prepared four ethanol bottles that contain pure ethanol, ethanol with 2wt% TriSilanol-Ph, ethanol with 2wt% TriSilanol-iBu, and ethanol with TriSilanol-Et respectively. Soak one aluminum 7075 T6 plate into each ethanol bottles for 24 hours and blow dry by Nitrogen gas before testing. Copper sample plates were prepared by the same procedure with aluminum 7075 T6 samples.

2.2.3 Contact Angle Measurements

Three droplets of 20 μ L DI water were dispensed by pipette (Eppendorf, Germany) onto each sample plate. The side-view, 45°-view images of droplets on plates were taken by Nikon D80 digital camera equipped with a one-to-one macro lens (Nikon, Tokyo). The sample plates were blow-dried and repeated the procedure of dispensing droplets and drying samples for three times. Contact angles were measured and labeled by NIS-Elements imaging software (Nikon Instrument, Inc). Each sample plate has a total of 9 contact angle measurements.

2.2.4 Aluminum/Copper Sample Powder Preparation

Powders of 30 μm 99.9% aluminum were soaked in 5 wt% HCl for 3 minutes at room temperature. The top supernatant acid solution was removed, and the aluminum powders precipitates were washed three times by DI water. Prepared four petri dishes that contain pure ethanol, ethanol with 2wt% TriSilanol-Ph, ethanol with 2wt% TriSilanol-iBu, and ethanol with TriSilanol-Et respectively. 5mg aluminum powder was added into each petri dish and was soaked for 24 hours before using. The preparation of copper powders followed the same procedure with aluminum powders, but three petri dishes that contain pure ethanol, ethanol with 2wt% TriSilanol-Ph, ethanol with 2wt% TriSilanol-iBu were prepared. 3g of copper powder was added into each ethanol mixture solution for surface treatment.

2.2.5 Hydrophobicity Test of Sample Powders

The aluminum and copper sample powders were washed by DI water multiple times to remove all the ethanol solution and then soaked into DI water at room temperature. The Al/Cu powders without TSP treatment were used as control samples. Images were taken by Nikon D80 digital camera.

2.2.6 Corrosion Tests of Copper Powders

The Cu sample powders were washed by DI water multiple times to remove all the ethanol solution and then soaked into 3.5 wt% sodium chloride solution at room temperature. The Cu powders without TSP treatment were used as control samples. Images were taken at the moment of as-soaked, 12-hour, 40-hour, 60-hour, 4-day, 6-day, 8-day ad 16-day by Nikon D80 digital camera.

2.2.7 Binary Aluminum Alloy and Aural 2 Sample Plates Preparation

Plates of 40 mm × 10 mm × 2.5 mm were cut by metal cut-off machine from the aluminum ingot and were well-polished that no scratch can be seen on the surface. The plate samples were cleaned by DI water and pure Ethanol washing.

2.2.8 Droplets Contact Area Measurements

Three droplets of 20 μL DI water were dispensed by pipette (Eppendorf, Germany) onto each sample plate. The top view of droplets on plates were taken by Nikon SMZ800N stereomicroscope (Nikon, Tokyo). The sample plates were blow-dried and repeated the procedure of dispensing droplets and drying samples for twice. The droplets contact areas were measured and labeled by NIS-Elements imaging software. Each sample plate has total of 6 contact area measurements.

2.3 Results and Discussions

2.3.1 Effect of Oxidation Layer on Aluminum Surface

To study the wettability performance of Aluminum 7075 T6 plate, the side-view images of the deionized water droplets on the plate immediately after polished and HCl etched and after exposing in the air for various length of time were taken. As Figure 4 shown, the based diameter of the droplets on Al plate decreases as the exposure time increases, which indicates that the Al 7075 T6 becomes more hydrophobic as the formation of the oxidation layer on the surface.



Figure 4. Side-view images of the water droplet on polished and HCl-cleaned Al plate exposed to air over 0 min, 1 min, 2 min, 4 min, 8 min, 16 min, 30 min, 60 min, and 6 hours.

2.3.2 Aluminum Substrates

Deionized water was used as the test liquid to examine the hydrophobicity of the aluminum powders. Figure 5 shows the images of the mixtures of aluminum powders and deionized water. Each petri dish in the photo contains 30 ml deionized water and 5 mg aluminum powders with and without TSP treatment. The majority of untreated Al powders sank into the bottom while all TSP-treated powders floated on the top, which means that Al powders become more hydrophobic after TSP treatment. No visible difference was observed among Et-TSP, iBu-TSP and Ph-TSP treated Al powders.

Contact angle testing was used to characterize the hydrophobicity of aluminum sheets with TSP dip coatings. The 45°-view images of Al sheets were taken with two droplets with different

volumes on the surface (Figure 6). The droplet on the left is 10 μL and the one on the right is 15 μL . Figure 7 shows the side-view images of Al sheets with three 20 μL water droplets on the top. The contact angles for all TSP-treated Al sheets were much larger than untreated sheets, which means that sheets became more hydrophobic after TSP treatment as well.

Hydrophobic performance of both aluminum powders and sheets improved after dip-coating with TSP, indicating that the TSP was grafted on the surface successfully.

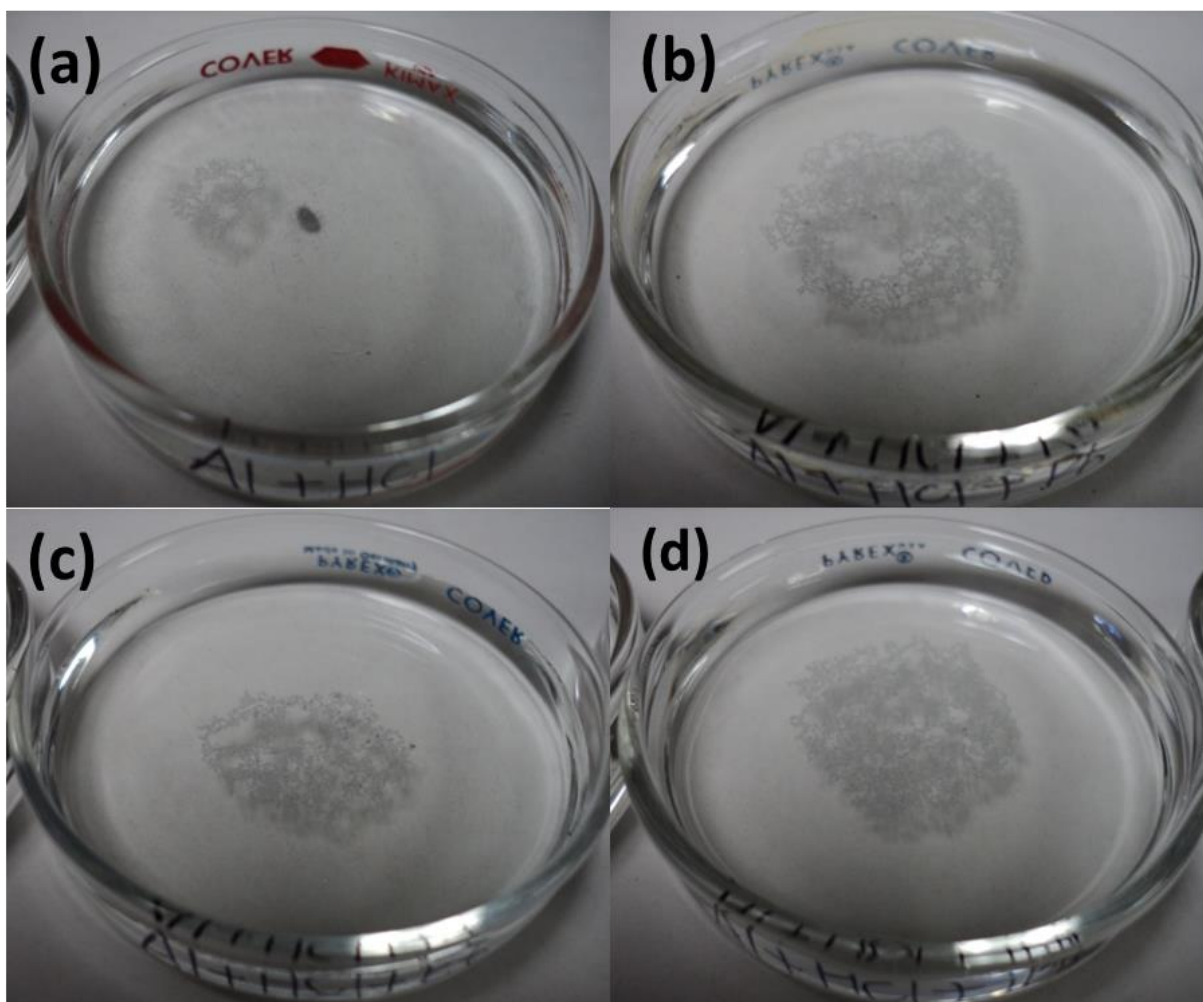


Figure 5. Images of 5mg Al powders soaked in 30 mL deionized water: (a) untreated Al, (b) Ph-TSP treated Al, (c) Et-TSP treated Al, and (d) iBu-TSP treated Al.

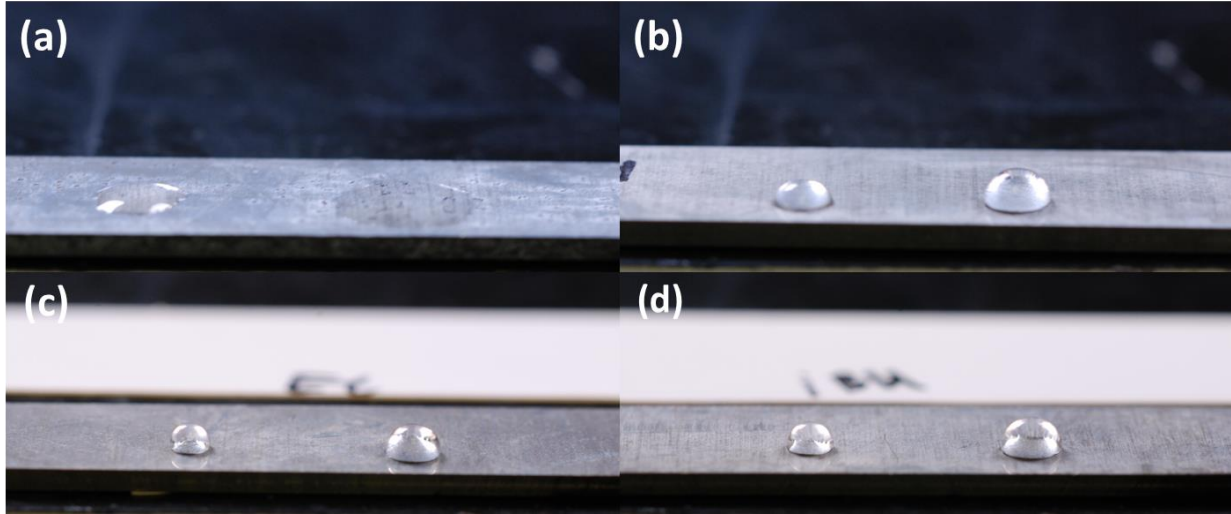


Figure 6. 45°-view images of Al sheet with two water drops on the top: (a) untreated Al, (b) Ph-TSP treated Al, (c) Et-TSP treated Al, and (d) iBu-TSP treated Al.

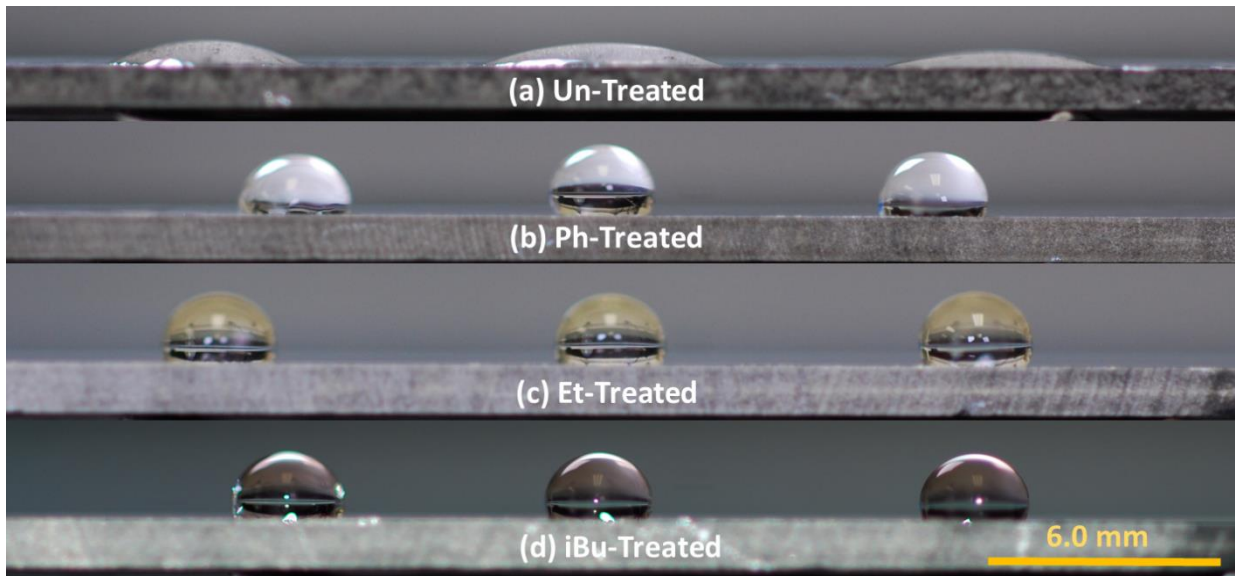


Figure 7. Side-view images of Al sheet with three water drops on the top: (a) untreated Al, (b) Ph-TSP treated Al, (c) Et-TSP treated Al, and (d) iBu-TSP treated Al.

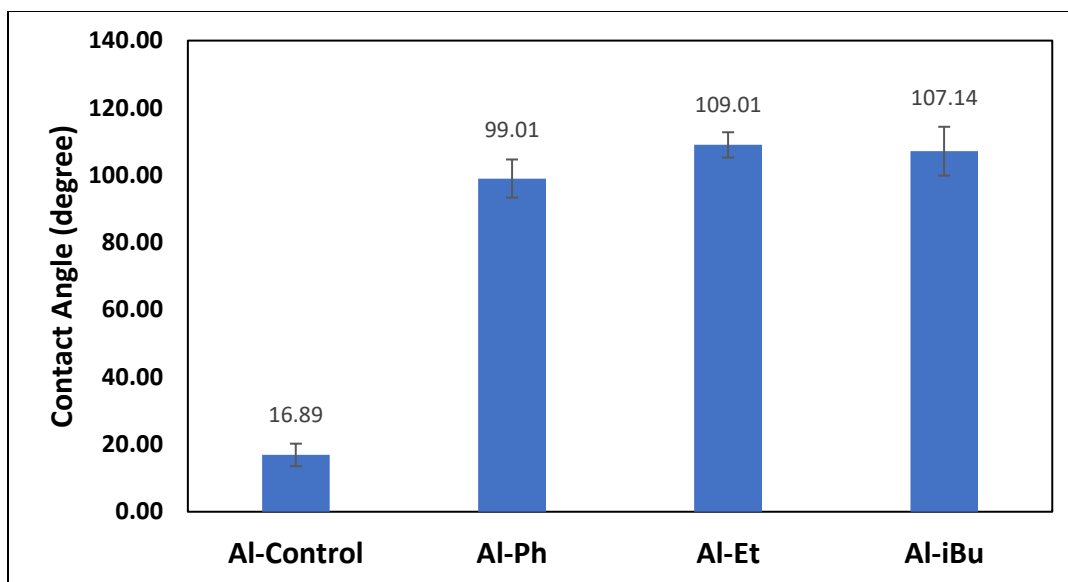


Figure 8. Contact angle measurements for untreated Al, Ph-TSP treated Al, Et-TSP treated Al, and iBu-TSP treated Al.

As Figure 8 shown, the Et-TSP treated aluminum plate has the largest contact angle, and untreated Al plate has the smallest contact angle. Contact angles of iBu-TSP treated Al plate and Ph-TSP treated Al plate are in between, and iBu-TSP treated ones have comparable larger contact angles.

To investigate the coating durability of different TSP coating, we carried out the experiment to test the contact angles right after coating, using Kimwipes (Kimberly-Clark) to clean the surface, and re-soaking the plate into pure Ethanol solutions for 5 days. Results for Ph-treated, Et-treated, iBu-treated samples are presenting in Figure 9, Figure 10 and Figure 11 correspondingly. From the results showing in all three figures, the changes in contact angles follow the same trend for all three types of treated samples. The physical cleaning by wiping the coated surface does not damage the coating significantly, but there exists a slightly decreasing of the contact angles, which means that the samples become more hydrophilic after physical cleaning. After re-soaking in the pure Ethanol solution, the reductions of contact angle are more obvious, and Ph-treat sample has the most dramatic reduction. From those results, we can tell that the

physical and chemical disturbance will affect the durability of TSP coating, but the physical wiping does not affect much, which is expected from chemical bonding.

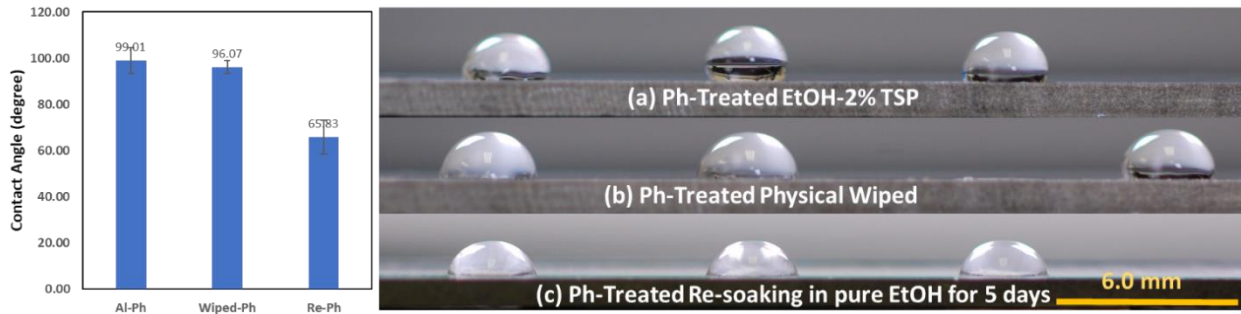


Figure 9. Contact angle measurements for Ph-TSP treated Al plate (a) soaked in 2% Ph-treated Ethanol (b) physically wiped (c) re-soaked in pure Ethanol for 5 days.

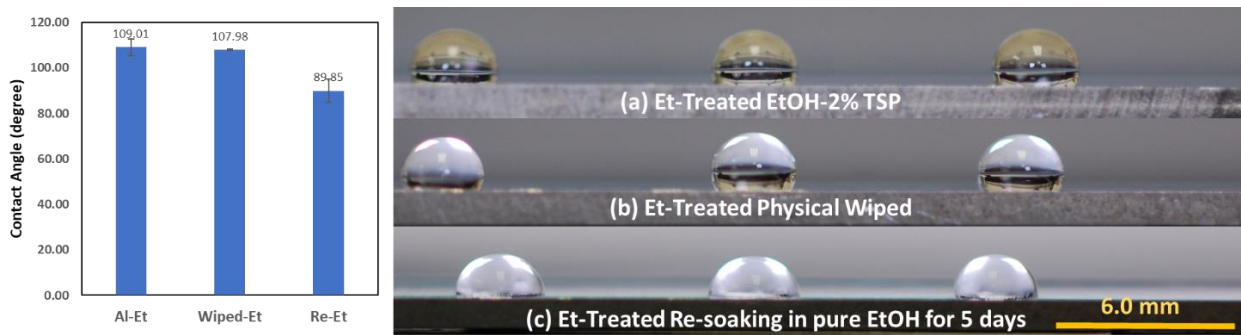


Figure 10. Contact angle measurements for Et-TSP treated Al plate (a) soaked in 2% Et-treated Ethanol (b) physically wiped (c) re-soaked in pure Ethanol for 5 days.

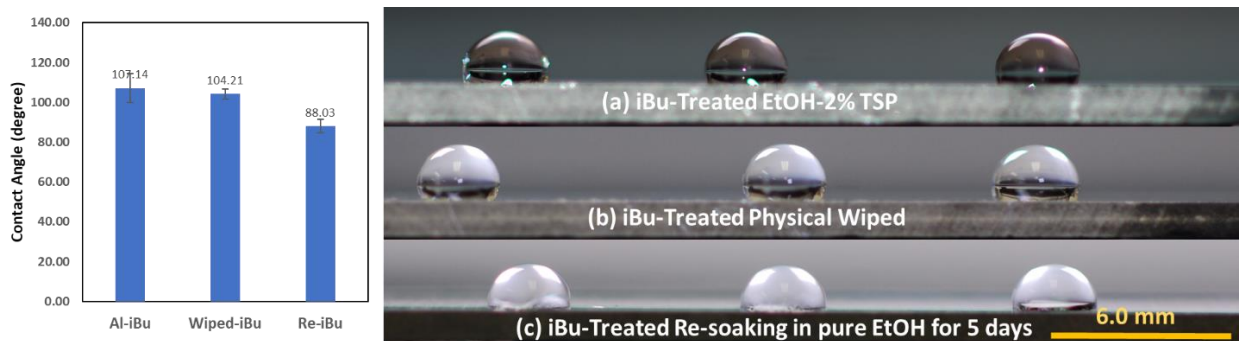


Figure 11. Contact angle measurements for iBu-TSP treated Al plate (a) soaked in 2% iBu-treated Ethanol (b) physically wiped (c) re-soaked in pure Ethanol for 5 days.

2.3.3 Copper Substrates

Deionized water was used as test liquids to examine the hydrophobicity of copper powders. Figure 12 shows the images of the mixtures of copper powders and deionized water. Each petri dish in the photo contains 30 ml deionized water and 3g copper powders with and without TSP treatment. Similar to the untreated aluminum powders, most of the untreated copper powders sank at the bottom with a small amount floated on the top (Figure 12a). However, TSP-treated copper powders sank at the bottom unlike TSP-treated aluminum. This happened because that copper has a much higher density (8.96g/cm^3) than aluminum (2.7g/cm^3), therefore, the weight of the copper powder is larger than the maximal buoyant force to hold it on the surface (Figure 12b and Figure 12c), while the weight of aluminum may be close to or smaller than the maximal buoyant force of the water surface. But the sunk TSP-treated copper aggregated together in the water by the cohesion force, and this phenomenon suggested that Cu shows hydrophobic behavior after TSP treatment. There was a trace amount of loosed iBu-TSP treated powders floating, while no Ph-TSP-treated powders were observed on top of deionized water.

To characterize the hydrophobicity of Cu sheets with TSP dip coatings, Figure 13 and Figure 14 shows the 45°-view and side-view images of Cu sheets with water droplets on top. As the same with the aluminum substrate, the 45°-view has two droplets which are 10 μL and 15 μL in volume and the side-view images were taken with three 20 μL droplets on the plates. From the images, we can tell that the contact angles for all TSP-treated Cu sheets are much larger than untreated sheets, which indicates that Cu sheets became more hydrophobic after TSP treatment.

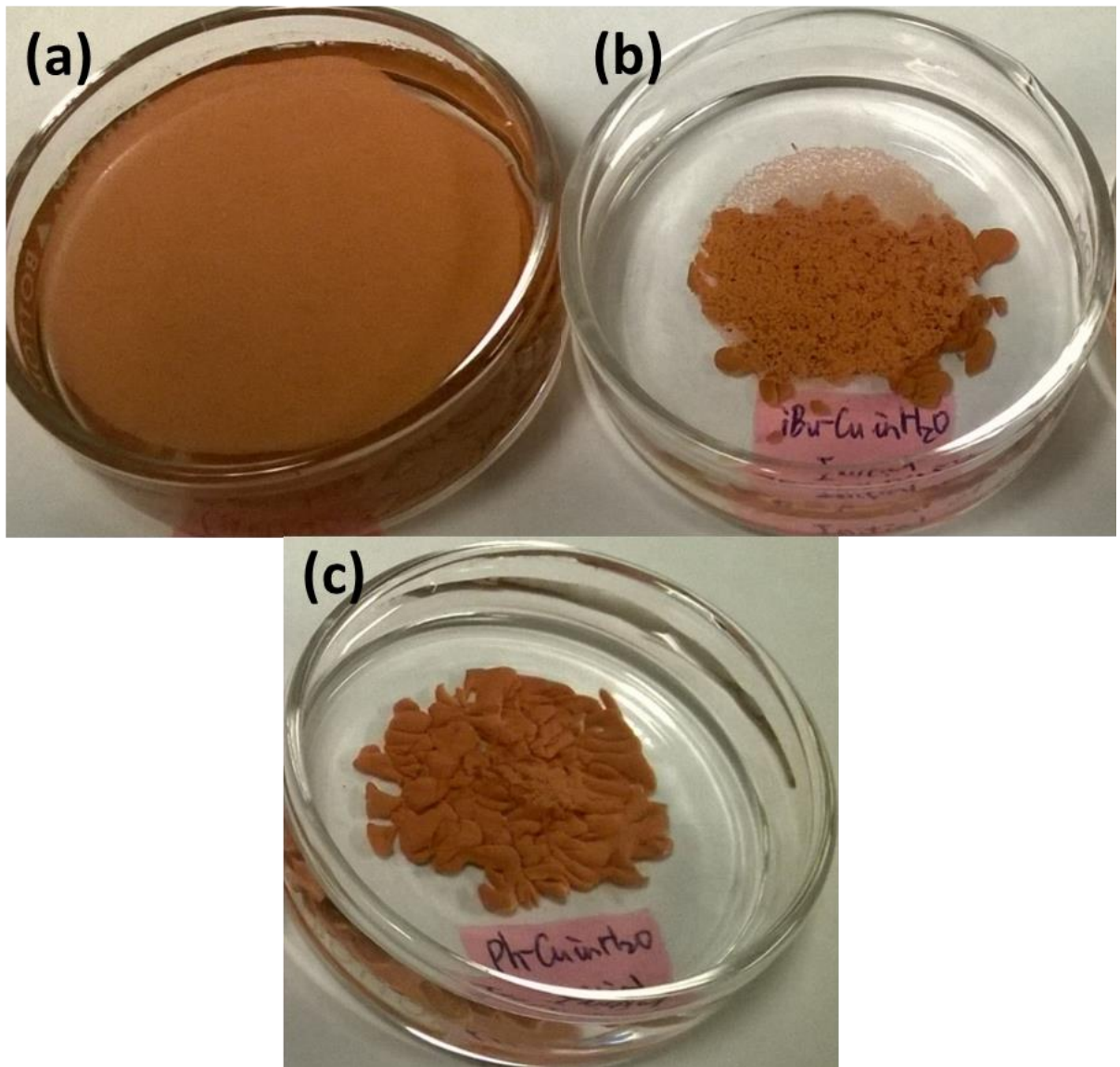


Figure 12. Images of 3g Cu powders soaked in 30 mL deionized water: (a) untreated Cu, (b) iBu-TSP treated Cu, and (c) Ph-TSP treated Cu.

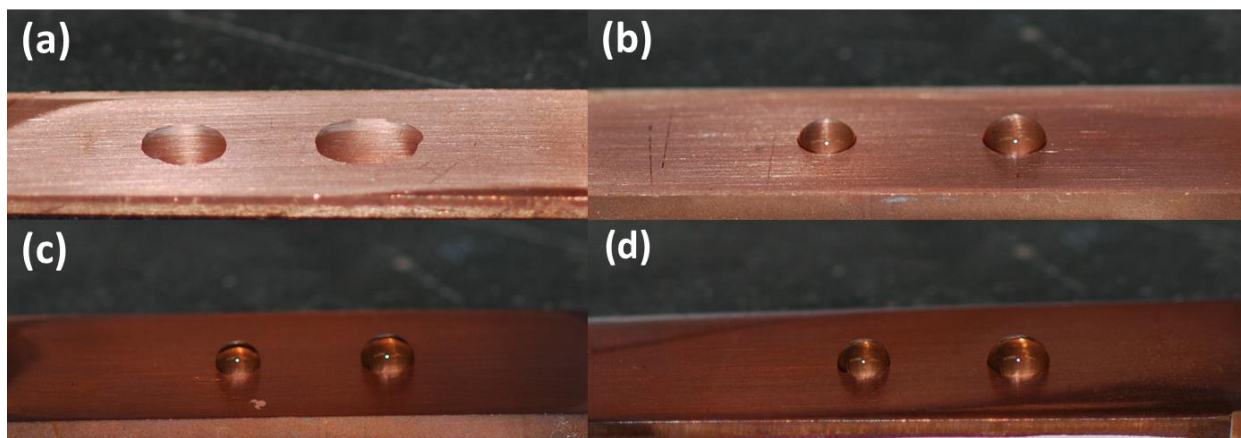


Figure 13. 45°-view images of Cu sheet with two water drops on the top: (a) untreated Cu, (b) Ph-TSP treated Cu, (c) Et-TSP treated Cu, and (d) iBu-TSP treated Cu.

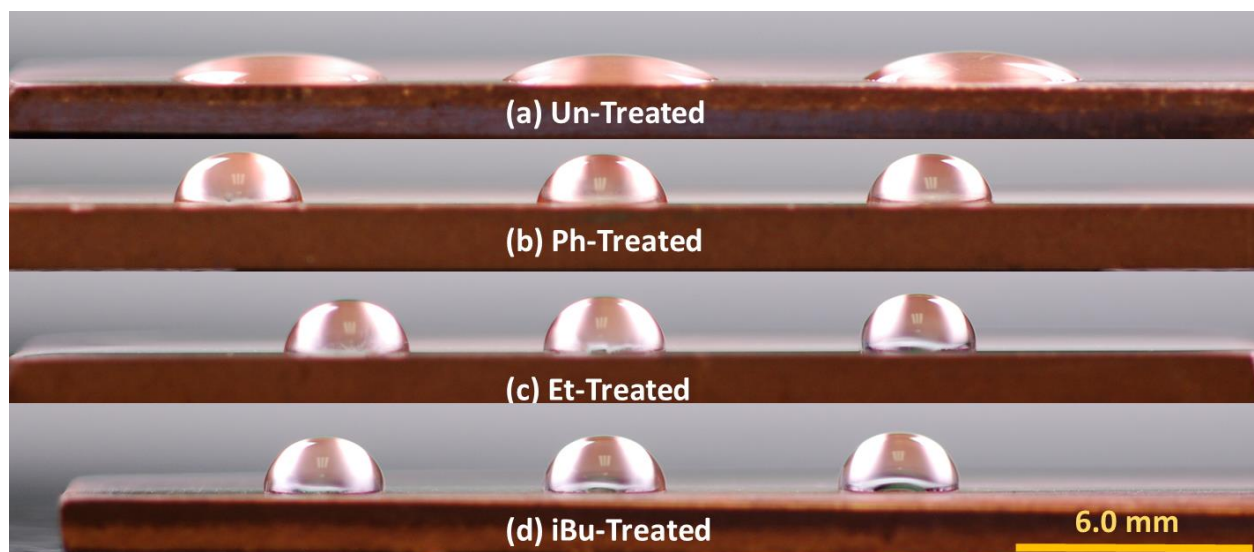


Figure 14. Side-view images of Cu sheet with three water drops on the top: (a) untreated Cu, (b) Ph-TSP treated Cu, (c) Et-TSP treated Cu, and (d) iBu-TSP treated Cu.

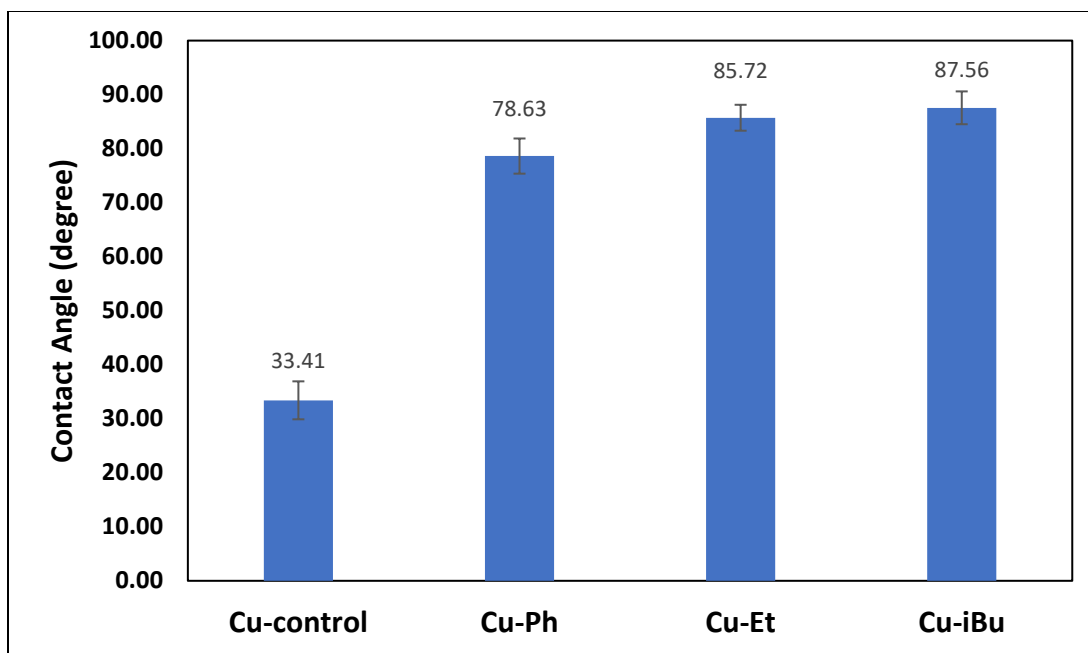


Figure 15. Contact angle measure for untreated Cu, Ph-TSP treated Cu, Et-TSP treated Cu, and iBu-TSP treated Cu.

Figure 15 shows the averaged contact angles for each sample. The untreated sample has the smallest contact angles, and all TSP-treated samples have much larger contact angles which are all above 78° . Within the treated samples, iBu-treated sample has the greatest contact angle and Ph-treated one has the smallest contact angles.

To further verify whether TSP was successfully grafted on the surface of Cu powders, corrosion tests were performed. All Cu powders were soaked in 3.5 wt% Sodium Chloride (NaCl) water for different periods of time. Figure 16 and Figure 17 show the soaked Cu powders in salt water for up to 16 days. Untreated copper powder turns a blue-green color after placing for 40 hours due to the formation of copper chloride as shown in Figure 16, and blue-green powders were formed after 60 hours and accumulated on the surface with the time in Figure 17. Copper chloride did not appear until 6-day soaking for both iBu-TSP and Ph-TSP treated powders. It took about 10 days to cover the entire surface for the TSP-treated copper while a large amount of copper chloride was deposited on the surface after only 1-2 days for untreated copper. The corrosion results suggest

that the anti-corrosion performance of copper powder is significantly improved after TSP treatment. TSP coatings were served as the barrier layer between corrosive medium and Cu substrate to prevent Cu from reacting with saltwater.

Both Cu powders and sheets became more hydrophobic after dip coating with TSP. In addition, TSP-treated Cu powders exhibited higher corrosion resistance than untreated powders. These results indicate TSP was grafted on the Cu surface successfully.

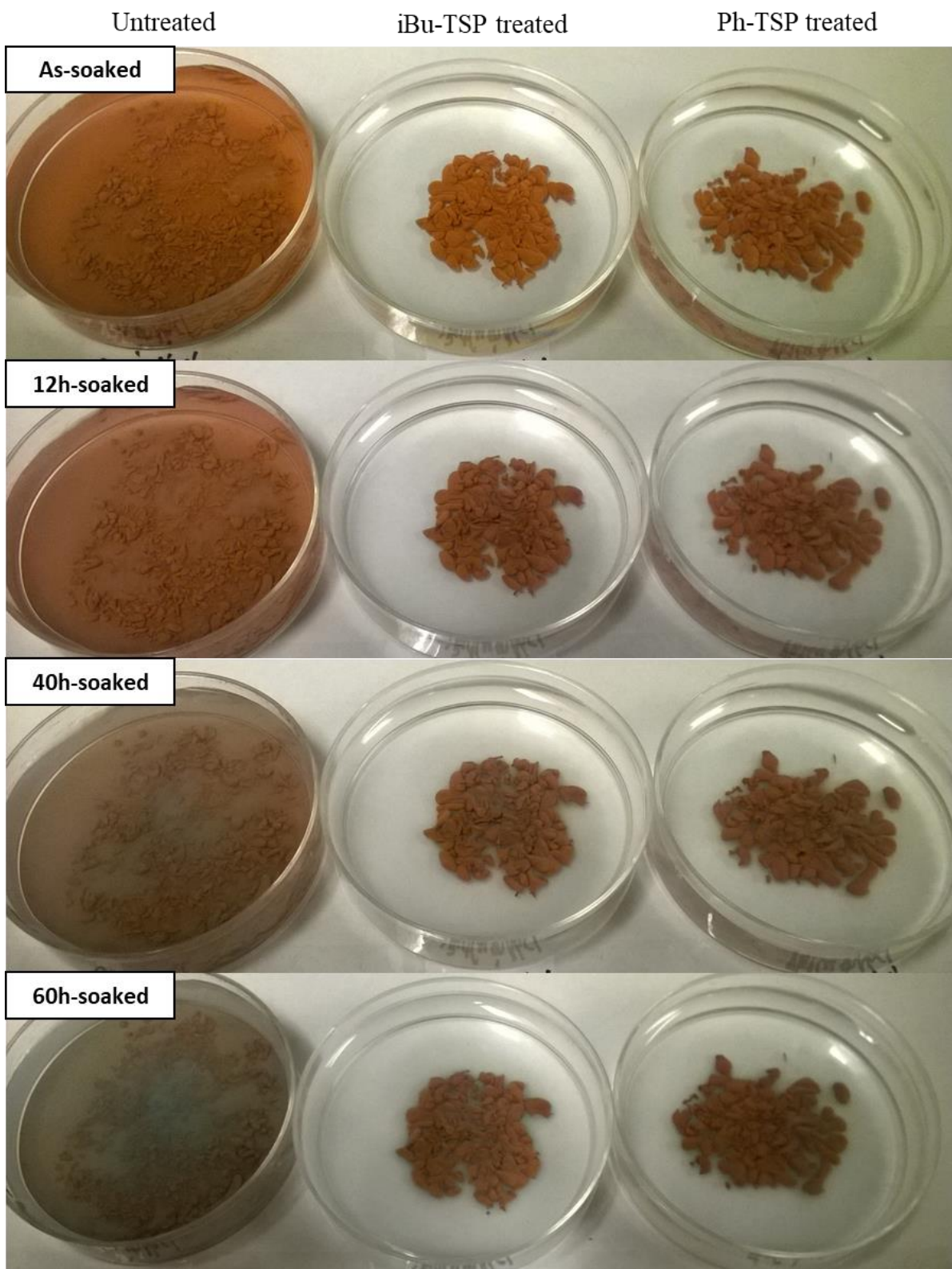


Figure 16. Images of 3g as received, iBu-TSP treated, and Ph-TSP treated Cu powders soaked in 30mL 3.5 wt% NaCl water up to 60 hours.

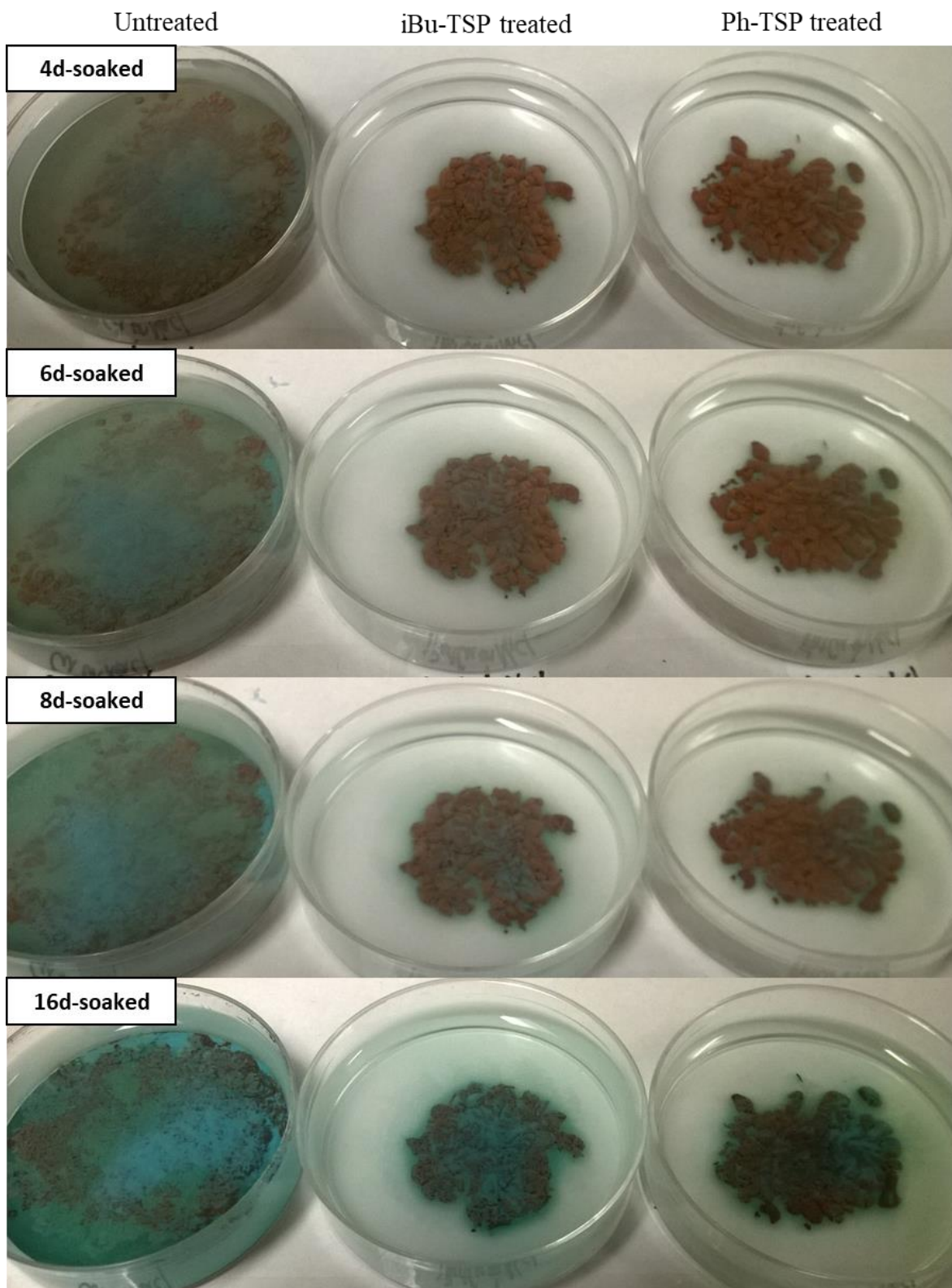


Figure 17. Images of 3g as received, iBu-TSP treated, and Ph-TSP treated Cu powders soaked in 30mL 3.5 wt% NaCl water from 4 days up to 16 days.

2.3.4 Modified Al-Alloy Substrates

In this section, we made two groups of casted aluminum alloys and compared the contact angles and contact areas for different modifications. Figure 18 and Figure 19 shows the side-view and top view of the droplets for Al-7.5Si binary alloy and Aural 2 alloy correspondingly. Figure 20 summarized the results for contact angles and contact areas for these two groups. From the result, we can see that the Sr-modified aluminum alloys will have larger contact angles than the TSP modified alloys, but the changes between the modified and unmodified alloys are not the same for two groups. For Al-7.5Si binary alloy, the untreated alloy plate has the largest contact angles and smallest contact areas, and TSP-treated alloy plate has the smallest contact angles and largest contact areas. But for Aural 2 alloy, the Sr-modified alloy has the largest contact angles and smallest contact areas while unmodified plates have the smallest contact angles and largest contact areas.

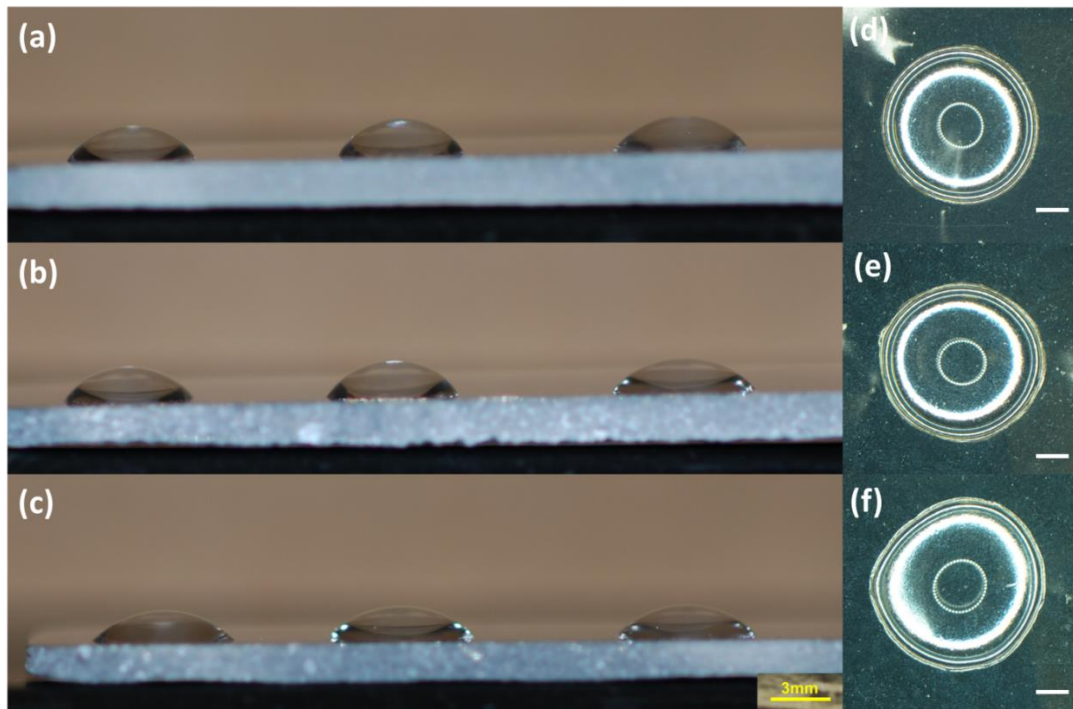


Figure 18. Side-view for (a) Al-7.5Si-untreated, (b) Al-7.5Si-TSP, and (c) Al-7.5Si-Sr. Top-view for (d) Al-7.5Si-untreated, (e) Al-7.5Si-TSP, and (f) Al-7.5Si-Sr.

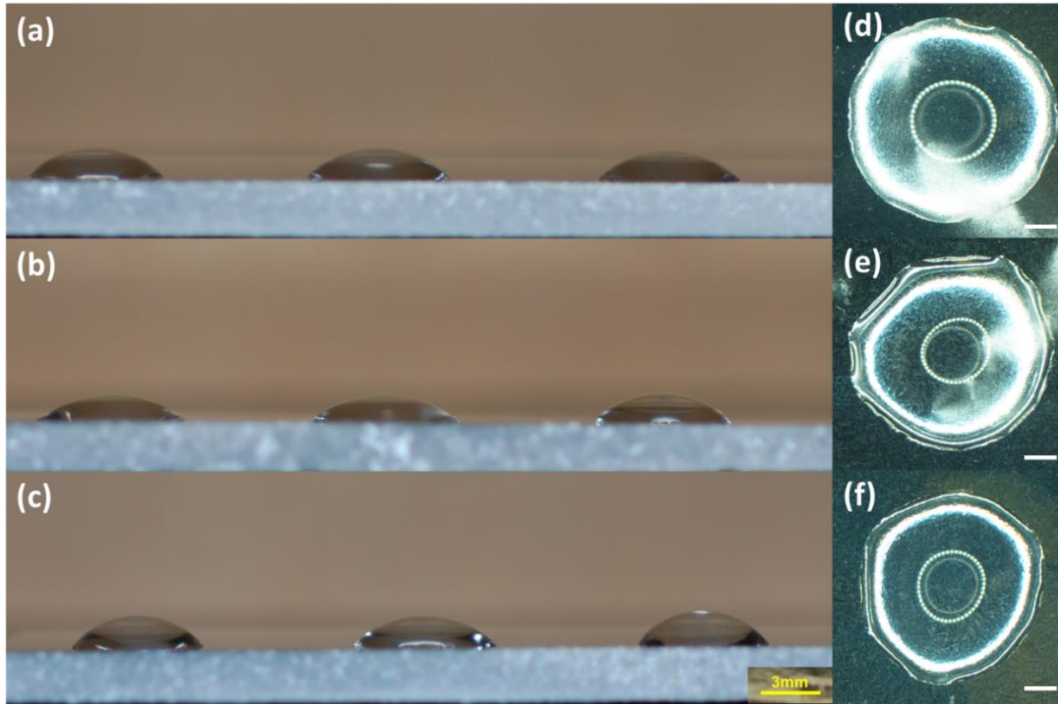


Figure 19. Side-view for (a) Aural 2 without Sr, (b) Aural 2 with TSP, and (c) Aural 2 with Sr. Top-view for (d) Aural 2 without Sr, (e) Aural 2 with TSP, and (f) Aural 2 with Sr.

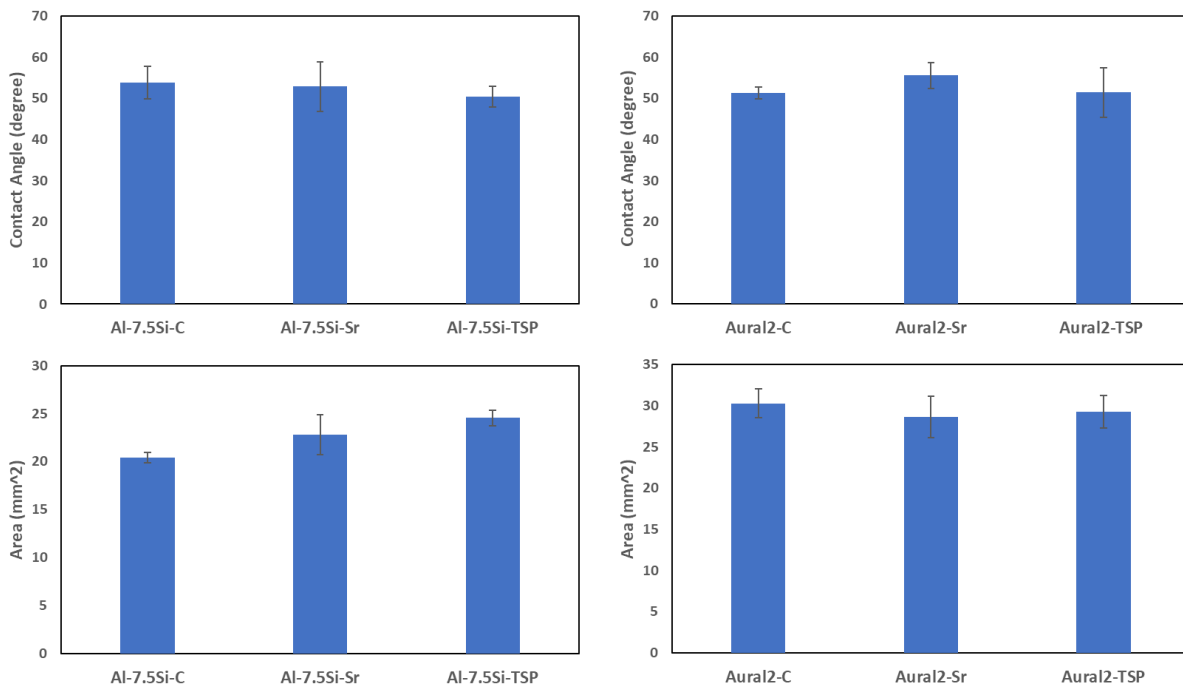


Figure 20. Contact angles measurements for Al-7.5Si alloy (top left) and Aural 2 alloy (top right); contact areas measurements for Al-7.5Si alloy (bottom left) and Aural 2 alloy (bottom right).

To better understand the changes in contact angles, we took scanning electron microscopy images for the group of Aural 2 alloys. As Figure 21 shown, under the same magnification, the unmodified deep-etched Aural 2 alloys has uniform pattern and dense microstructure, while the TSP modified alloy has similar microstructure shape but more dense patterns. However, for Sr-modified samples, the larger microstructures with more rough edge make it quite different from the other two. Therefore, the contact angles of the unmodified samples are similar to the TSP modified samples, but the smallest microstructure pattern makes TSP-modified alloy the smoother surface and smaller contact angles than the other two samples.

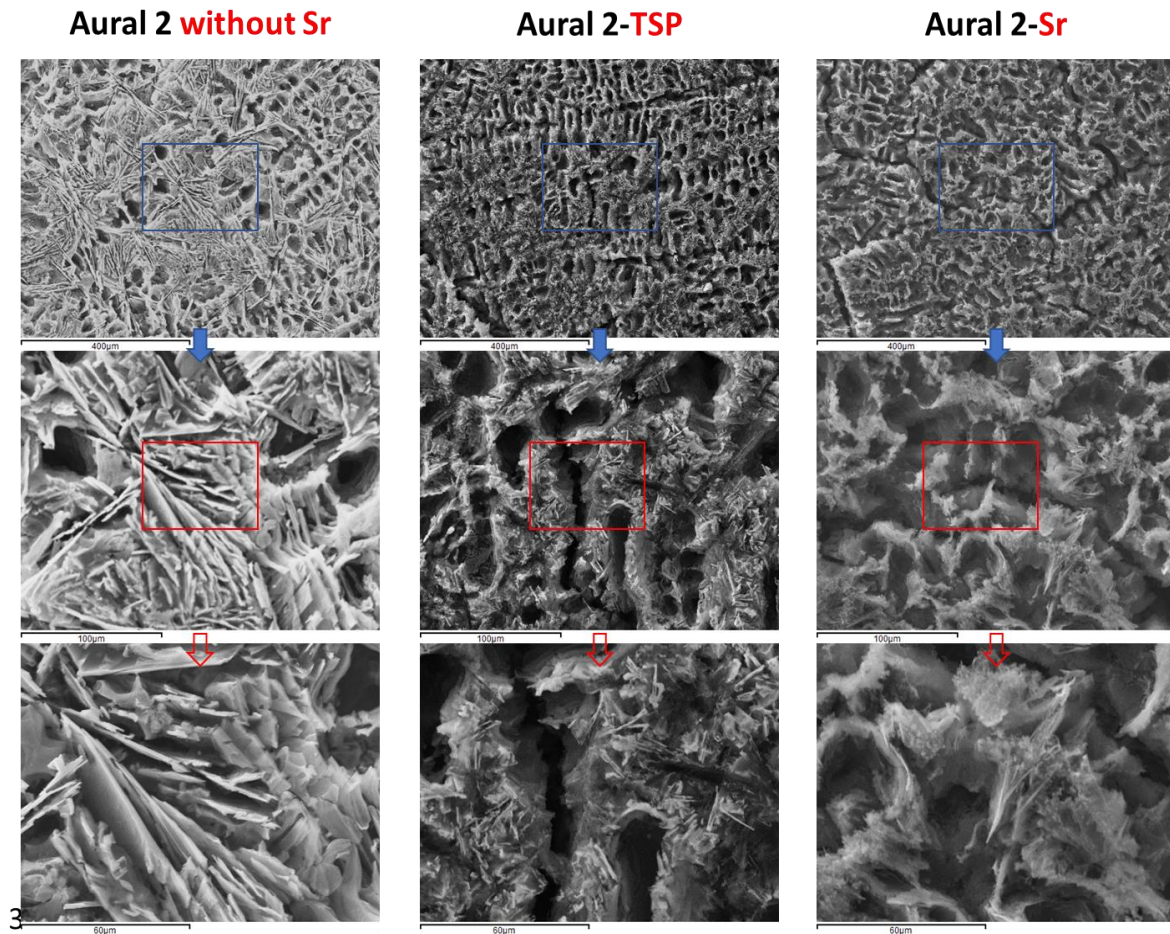


Figure 21. SEM Micrographs of the Deep-etched Aural™ 2 Alloys: (a) Aural™ 2 Base, (b) Aural™ 2 with TSP, and (c) Aural™ 2 with Sr. [2]

2.4 Conclusions

In this section, we have done droplet contact angles tests for several materials under various conditions. Initially, we investigated the effects of oxidation layer for the hydrophobic performance, and from the result we can tell that the untreated polished Al 7075 T6 plates have very small contact angles after HCl cleaning, and the contact angles increases as the oxidation layer growing on the surface. Although the contact angles are getting larger as the exposure time in air increases, they are still smaller than 20° after the oxidation layer is formed on the surface after 6 hours. Therefore, the growth of the oxidation layer has limited contribution ($\sim < 10^\circ$) to the dramatic increase in contact angles for different treatment since the experiments were done within one hour after getting the sample out of the treated solution or after polished and HCl cleaning. Secondly, we have investigated the hydrophobicity of powder forms Al and Cu by soaking a certain amount of untreated and treated powders in different petri dishes with 30mL deionized water, and we can tell that the TSP-treated samples became more hydrophobic by either floating on the water surface or aggregate together when sinking to the bottom. For the samples made by coating different TSP, the contact angles are significantly increased for both Al and Cu samples for all three different TSP treatment. To further investigate the durability of the TSP coating for Al samples, we also tried with physically wiped by tissue papers and pure ethanol solution soaking for 5 days, and we discovered that the physically wiping will not damage the surface but the re-soaking in pure ethanol solution will reduce the contact angles. For the Ph-TSP treatment sample, the effect of re-soaking in pure ethanol is significant, which is around 34° decreasing, but the Et-TSP and iBu-TSP treated samples only have around 20° decreasing. For Cu samples, the contact angles after coating are similar for Et-TSP and iBu-TSP treated, but the Ph-TSP treated samples have smaller contact angles compared to the other two, but still much larger than the untreated Cu

samples. From the 3.5wt% NaCl water corrosion experiment for Cu powder, we can tell that the TSP coating created a barrier between the solution and powder which help the material to resist the corrosion from the saltwater. Lastly, by measuring the contact angles of the modified samples, we noticed that contact angles would not be affected much by the modification. For the Al-7.5Si, the modified samples will have slightly smaller contact angles, but for Aural 2 samples, the modified samples will have slightly larger contact angles. We also took SEM images for the Aural 2 samples, and the differences of microstructure of the Aural 2 support the contact angle performance.

CHAPTER 3 EFFECT OF MICROSTRUCTURE ON POLARIZATION BEHAVIOR OF AL-SI BASED CASTING ALLOYS

3.1 Introduction

In this chapter, we talked about the polarization behavior of Al-Si based casting alloys. The open circuit measurement and the potentiodynamic polarization measurement were carried out to investigate the corrosion behavior of three types of materials, which are Al-7.5Si, Aural 2 alloy and W319 base alloy. For each group of the results, the polarization curves, corrosion current density and open circuit potential measurement results were listed. The anodic current density cannot be determined accurately since the curve of the anodic branch goes up so fast where the linear region cannot be seen on the polarization curve.

3.2 Materials and Methods

3.2.1 Sample preparation

There are three major groups of Al-alloy involved in this study, which are all made by Dr. Yang Lu from Michigan State University (East Lansing, MI). The first group is Al-7.5Si; the second group is Al-7.5Si-3Cu-0.2Mg-0.1Ti-0.1Fe (W319 base alloy); the third group is Al-11Si-0.3Mg-0.5Mn-0.2Fe (Aural 2 alloy). Each group of Al-alloy has control sample, TSP-treated sample and Sr-treated sample. The ingots of these three groups were prepared individually. Epoxy Kit with 2 epoxy compounds (Epoxy Resin (QC) and Epoxy Hardener (QC)) was bought from LECO corporation (ST. Joseph, MI). All sample ingots were cut into 30 mm × 5 mm × 4 mm plates and prepared by encapsulating the sample ingot in an epoxy-based molding compound. Part of the sample remained unencapsulated to be connected with the working electrode (WE) lead from the VSP-300 potentiostat machine (Bio-Logic Science Instruments, France). The sample was encapsulated as Figure 22. After the encapsulation, the bottom was ground and well-polished to expose the sample surface. The polished surface was cleaned in the soapy water using an ultrasonic

bath followed by a thorough wash using the deionized (DI) water. The prepared WE surface was dried in air and the area of the exposed surface was measured before each test.

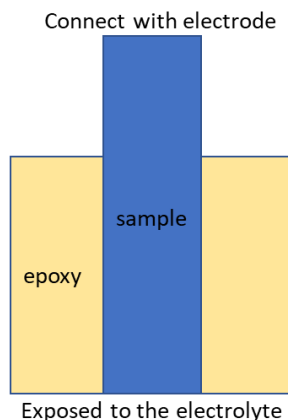


Figure 22. Schematic illustration of sample encapsulation.

3.2.2 Electrochemical Characterization

Open circuit potential measurements, anodic and cathodic polarization measurements were used in this study to characterize the self-corrosion behavior of a metallic entity.

3.2.3 Electrode Preparation

The prepared sample was used as the working electrode (WE) lead in the potentiostat. The counter electrode (CE) is made of platinum foil (99.95% metals basis) with 25 mm × 12 mm × 0.25 mm. The reference electrode (RE) is accumet™ (Fisher Scientific, USA) standard electrode with the Ag/AgCl immersed in saturated Potassium Chloride (KCl) solution.

3.2.4 Electrolyte Preparation

In order to study Al corrosion behavior applied at the automotive industry, chloride is the primary corrosive species in the molding compound [13] with a high concentration. Appropriate amounts of sodium chloride (NaCl) obtained from Barnstead Nanopure™ was dissolved in DI water ($\approx 18 \text{ M}\Omega \cdot \text{cm}$). The water extract of commercialized epoxy-based molding compounds have a conductivity equivalent to a pH 6.4, 10,000ppm NaCl solution at room temperature ($\sim 25^\circ \text{C}$).

3.2.5 Open Circuit Potential Measurement

The potentiostat was used to carry out all the electrochemical measurements. Open-circuit potential (E_{oc}) is the potential difference between the WE and the RE, and it indicates the nobility of metal. A metal with a higher value of E_{oc} is less likely to be corroded [14]. A two-electrode configuration was used for the E_{oc} measurement as shown in Figure 23 without using the counter electrode. To obtain a stabilized value of E_{oc} , the working electrode was immersed in the electrolyte for an extended period of time [14]. The length of the immersion varied depending on the type of the WE. Aluminum requires a longer time for its E_{oc} value to stabilize due to the properties of a passivating metal. The E_{oc} measurement is sensitive to the surface condition of the sample [15]. A long immersion time (72 hours) in 1ppm NaCl electrolyte for Al is required due to the slow passivation process on its surface [15]. The $E_{oc,Al}$ value fluctuates as the Al surface is being passivated and the E_{oc} value will not stabilize until a mature passive film forms on the Al surface. However, since the solution condition is applied to vehicle, the concentration of NaCl solution is high (10000 ppm). Therefore, the passivation process is much faster than concentration of 1 ppm. In this study, the immersion time for Al was 1 hour, and the E_{oc} was monitored within this period of time with the stabilized E_{oc} values reported.

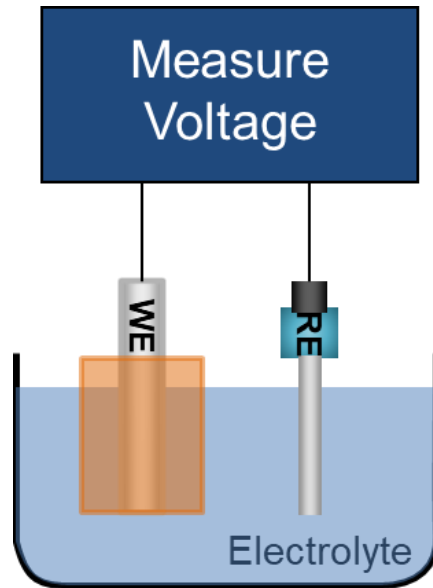


Figure 23. Two-electrode configuration for the Open Circuit Potential Measurement.

3.2.6 Potentiodynamic Polarization Measurement

After a stable E_{oc} was obtained following the ASTM G5-14 Standard [16], the potentiodynamic polarization measurements were carried out. The three-electrode configuration as shown in Figure 24 was used. The potentiostat measures $E_{measured}$, which is the potential between the RE and the WE, while applying a current (I) between the CE and the WE. As shown in equation (1), the value of $E_{measured}$ is the sum of the applied potential (E_{WE}) on the WE, and the ohmic potential drop (IR_{soln}) due to the electrolyte resistance between the WE and the RE [17]:

$$E_{WE} = E_{measured} - IR_{soln} \quad (1)$$

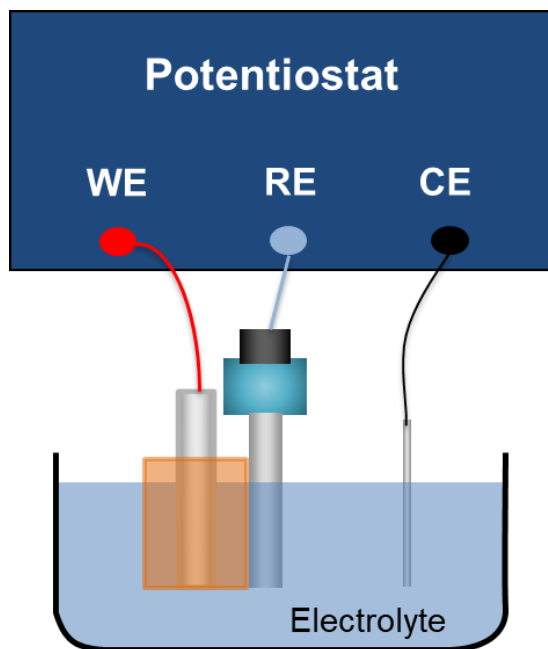


Figure 24. Three-electrode configuration for the potentiodynamic polarization measurements.

The distance between the RE and the WE were minimized, and the electrolytes used in this study have high concentrations of NaCl with low resistivity. Therefore, the R_{soln} value in Eqn. 1 will be extremely small, which is negligible.

3.3 Results and Discussions

The major difference between the three modified Al casting alloys is the Si content. Their anodic and cathodic polarization curves were measured in 1 wt% NaCl solution and plotted together in Figure 25. For all the alloys studied, the cathodic current density was not significantly affected by the applied potential, indicating that the oxygen reduction reaction predominantly controlled by the oxygen diffusion in the solution. The anodic current density increased rapidly with the increasing applied potential before it approached the diffusion-controlled regime like the cathodic branch. The rapid increase in the anodic current density indicated that these alloys were undergoing pitting corrosion even under the open circuit potential. Both Al-7.5 Si and W319 base alloy exhibited a lower anodic current density and a higher cathodic current density than Aural 2

alloy. Therefore, the E_{oc} values of Al-7.5 Si and W319 base alloy were higher than that of the Aural 2 alloy. The anodic current density of the Al-7.5 Si and W319 base alloys were lower than that of the Aural 2 alloy (Figure 25), this is consistent with the literature that shows the higher Si content in the Al casting alloys leads to a higher anodic current density [18]. The corrosion current densities of the Al-7.5 Si and W319 base alloys were slightly higher than that of the Aural 2 alloy due to their higher cathodic current density (Figure 26a). Figure 26b shows that the potential applied on the working electrode has the similar relationship with the cathodic current density among these three alloys, where the W319-base alloy has a much higher potential applied than the other two.

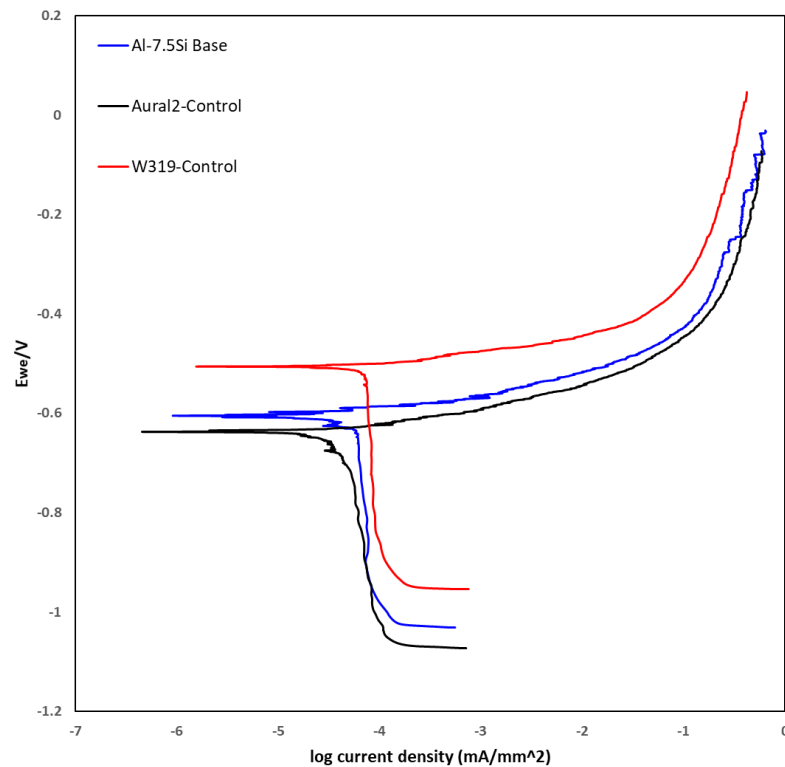


Figure 25. Polarization curves of Al-7.5Si Base, Aural2-Control, and W319-Control in an electrolyte solution containing 1wt% NaCl.

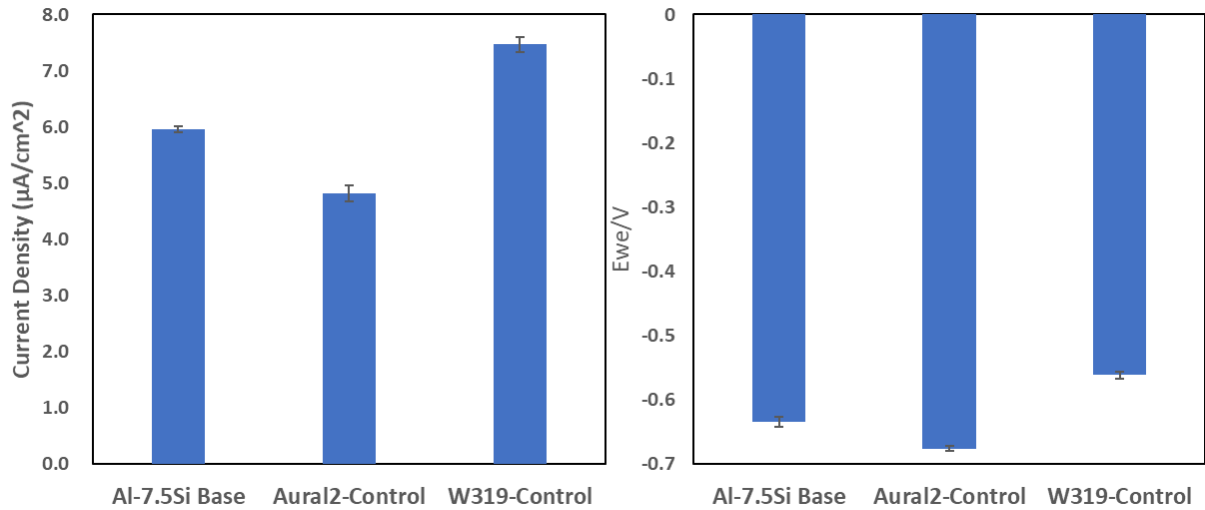


Figure 26. (a) Corrosion current density and (b) open circuit potential measurement of Al-7.5Si Base, Aural2-Control, and W319-Control.

The polarization curves of Al-7.5Si casting alloy with and without Sr modification were measured in 1 wt% NaCl solution as well and plotted in Figure 27. Both the anodic and cathodic polarization behavior was not changed with the Sr modification. This indicates that adding Sr can refine the microstructure of the Al casting alloy (from plate-like structure to the needle-like structure as shown in the previous chapter) without significantly increasing the corrosion rate (Figure29), which is beneficial since it has been reported that refined microstructure is always associated with an increased corrosion rate. [19] As compared with Sr, TSP as a microstructure modifier can provide much more benefits. The polarization curves of Al-7.5Si casting alloy with TSP modification was measured in 1 wt% NaCl solution and plotted in Figure 27 as well. Similarly, both the anodic and the cathodic polarization behavior were not significantly changed by the TSP addition. The polarization curves of Al-7.5Si alloy modified with different amount of TSP (0.5% and 1%) were shown in Fig 29. This also confirmed that the polarization behavior of Al-7.5Si alloy did not change with the TSP modification regardless of the amount of TSP added. The current densities for a different amount of TSP adding were almost the same as well as the potential applied

(Figure 30). The reason that both Sr and TSP modification did not change the polarization behavior might be due to the electrochemically-inert nature of Si.

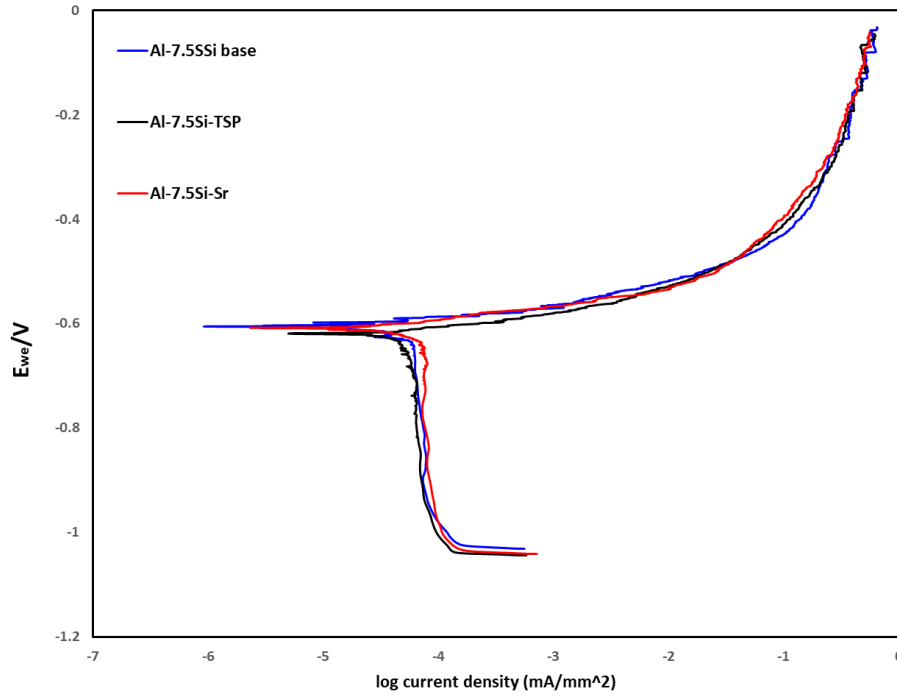


Figure 27. Polarization curves of Al-7.5Si Base, Al-7.5Si-TSP, and Al-7.5Si-Sr in an electrolyte solution containing 1wt% NaCl.

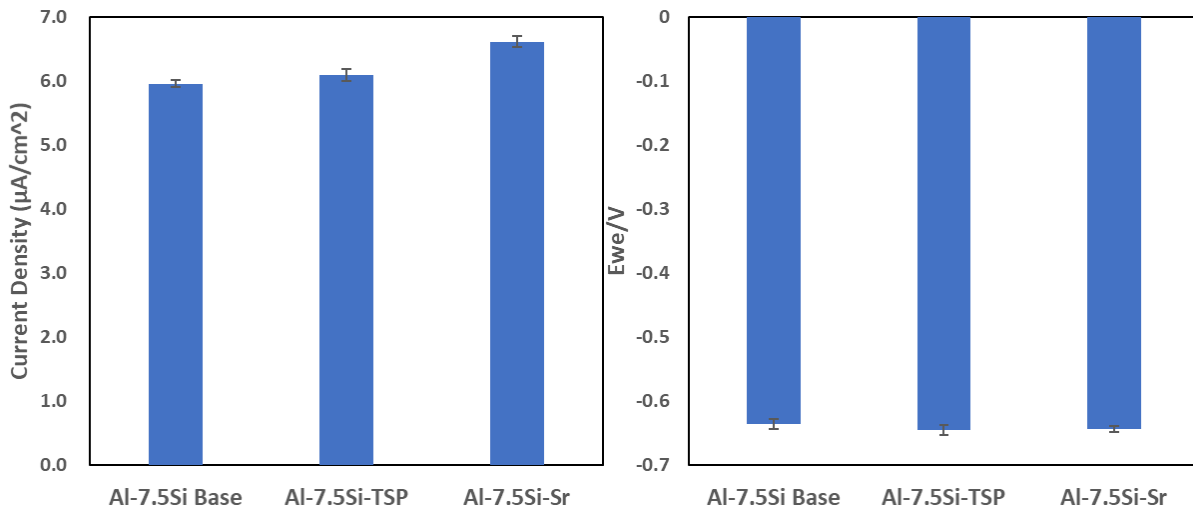


Figure 28. Corrosion current density and open circuit potential measurement of Al-7.5Si Base, Al-7.5Si-TSP, and Al-7.5Si-Sr.

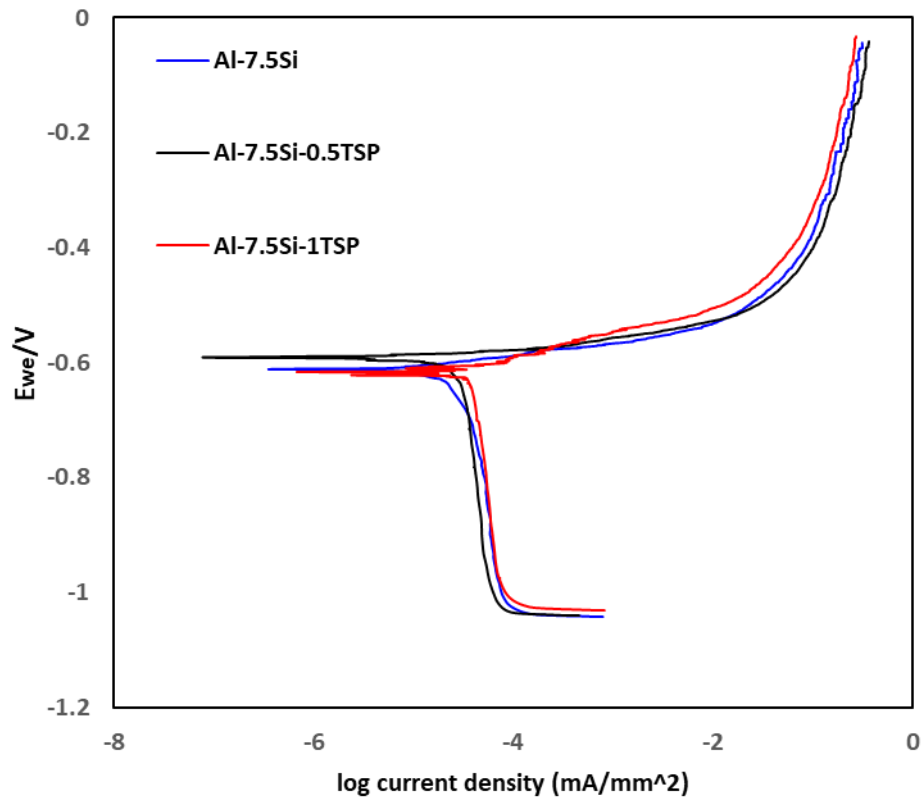


Figure 29. Polarization curves of Al-7.5Si, Al-7.5Si-0.5TSP, and Al-7.5Si-1TSP in electrolyte solution containing 1wt% NaCl.

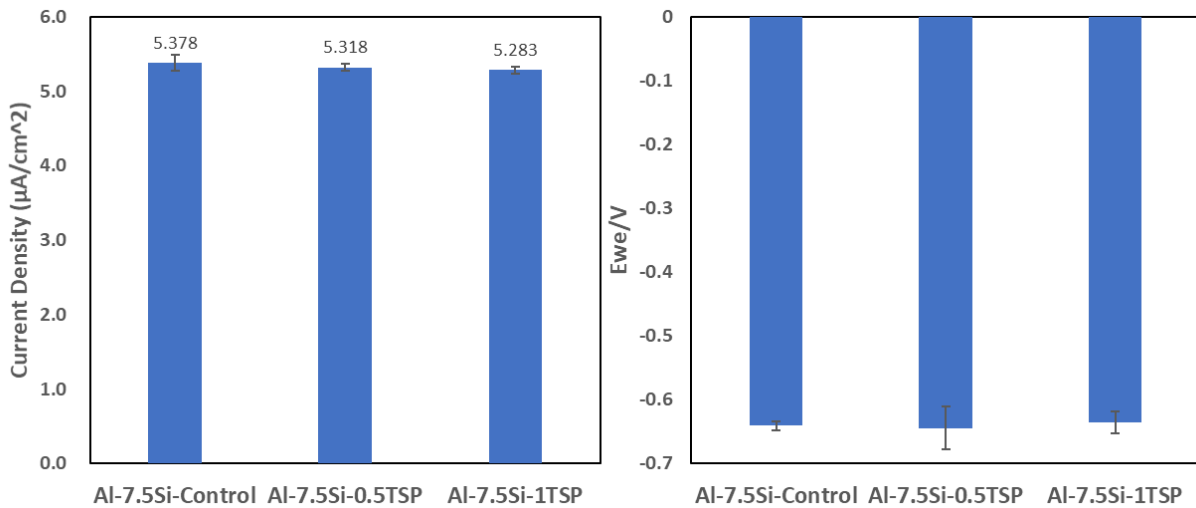


Figure 30. Corrosion current density and open circuit potential measurement of Al-7.5Si, Al-7.5Si-0.5TSP, and Al-7.5Si-1TSP.

The polarization curves of W319 casting alloy and Aural 2 alloy with and without TSP modification were measured in 1 wt% NaCl solution as well and plotted in Figure 31 and Figure 33 respectively. Like Al-7.5Si alloy, the polarization behavior of W319 casting alloy did not change with the TSP modification (Figure 33). However, a decrease in the anodic current density with the microstructure modification was observed for Aural 2 alloy (Figure 34). Both Al-7.5Si and W319 casting alloy are hypo-eutectic Al alloy, while Aural 2 alloy is near eutectic. The microstructure refinement majorly occurred to the eutectic phase instead of the primary Al phase. Thus, it is expected that the microstructure of Aural 2 alloy would be refined to a much higher degree than that of the other two hypo-eutectic alloys. The electrochemically active elements such as Mg, Fe, present in the Aural 2 alloy matrix can form intermetallics with Al and participate in the Al matrix. These intermetallics can form micro-galvanic cells with the surrounding Al. Based on the anodic polarization curve, the microstructure refinement increased the density of these micro-galvanic cells. As the galvanic corrosion occurs, the dissolved Al ions redeposited on the Al alloy surface and form insoluble Al oxide. Al oxide can passivate the surface and inhibit further corrosion. As the micro-galvanic cells become denser and smaller with the microstructure refinement, the Al oxide is more compact and passive. This contributes to the observed lower anodic current density as the surface is being anodically polarized.

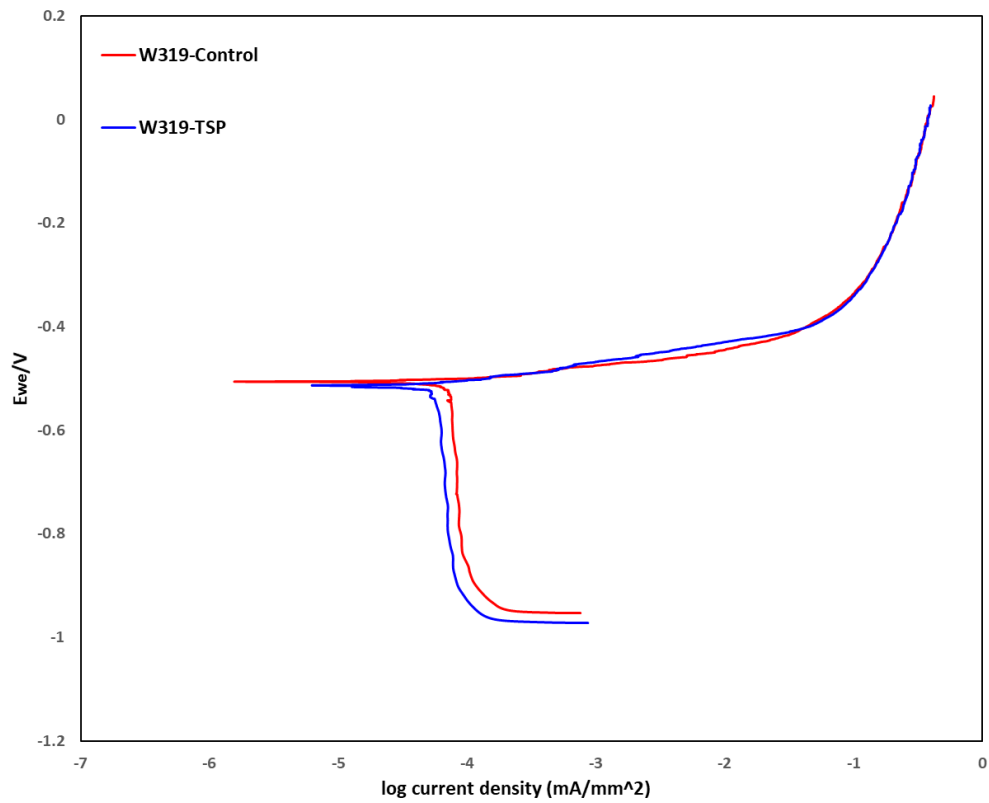


Figure 31. Polarization curves of W319-Control, and W319-TSP in an electrolyte solution containing 1wt% NaCl.

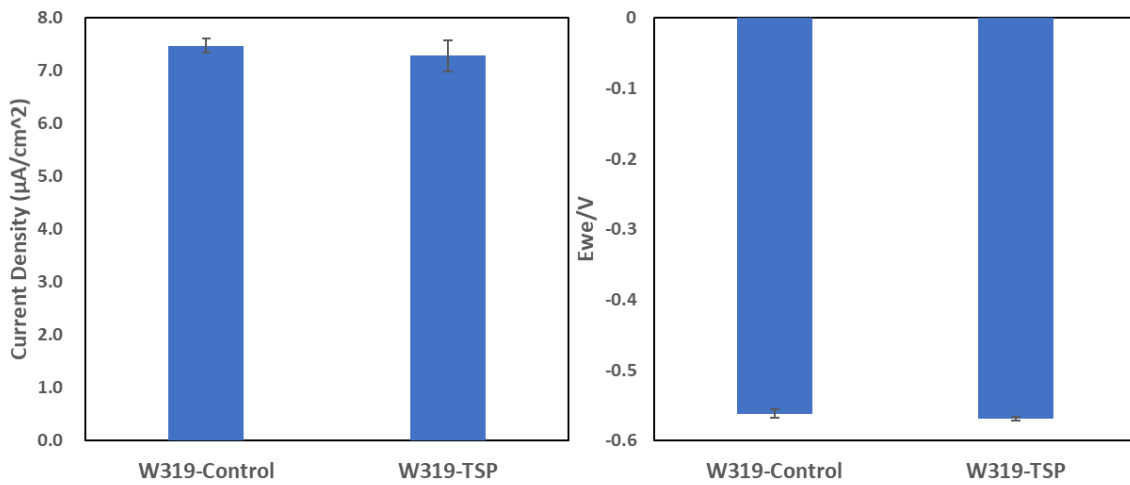


Figure 32. Corrosion current density and open circuit potential measurement of W319-Control, and W319-TSP.

The polarization curve of Aural 2 alloy with Sr modification was measured in 1 wt% NaCl solution and plotted in Figure 33 as well. The microstructure is more refined with Sr as compared with TSP. Thus, the anodic current density of Sr-modified Aural 2 alloy is lower than that modified with TSP alloy (Figure 34). This further confirmed that a refined surface structure could be more easily passivated.

It can be concluded that the microstructure refinement with Sr or TSP does not have a significant effect on the corrosion behavior on the hypo-eutectic Al alloy, however, reduce the anodic current density of the eutectic Al alloy due to a higher degree of the eutectic structure refinement.

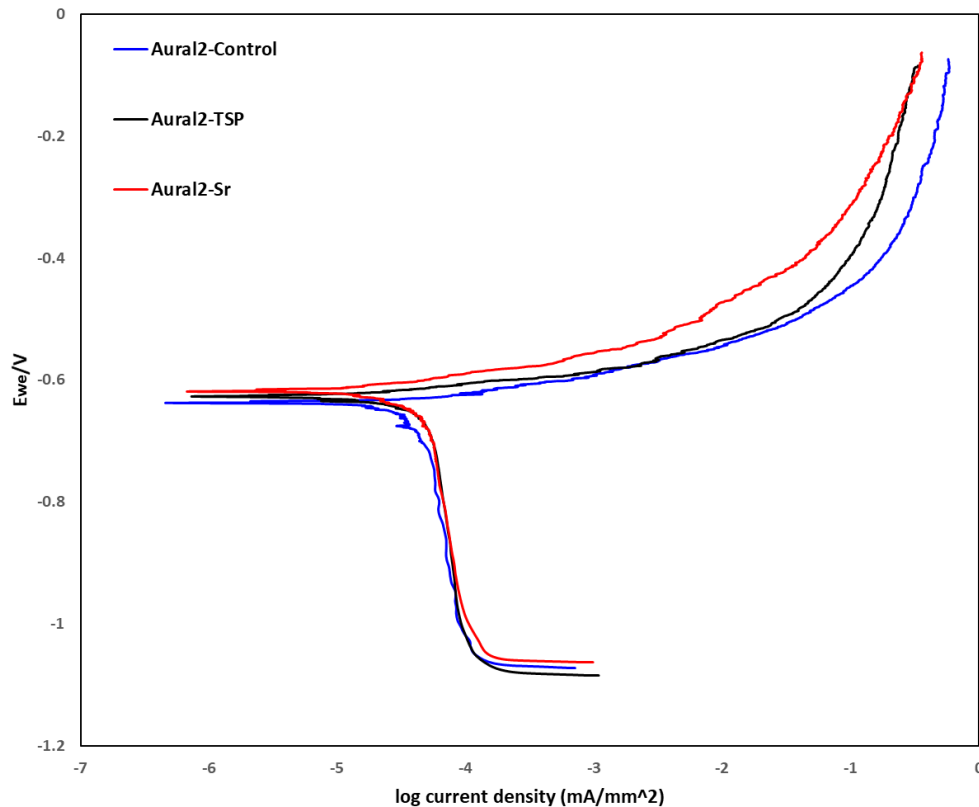


Figure 33. Polarization curves of Aural2-Control, Aural2-TSP, and Aural2-Sr in an electrolyte solution containing 1wt% NaCl.

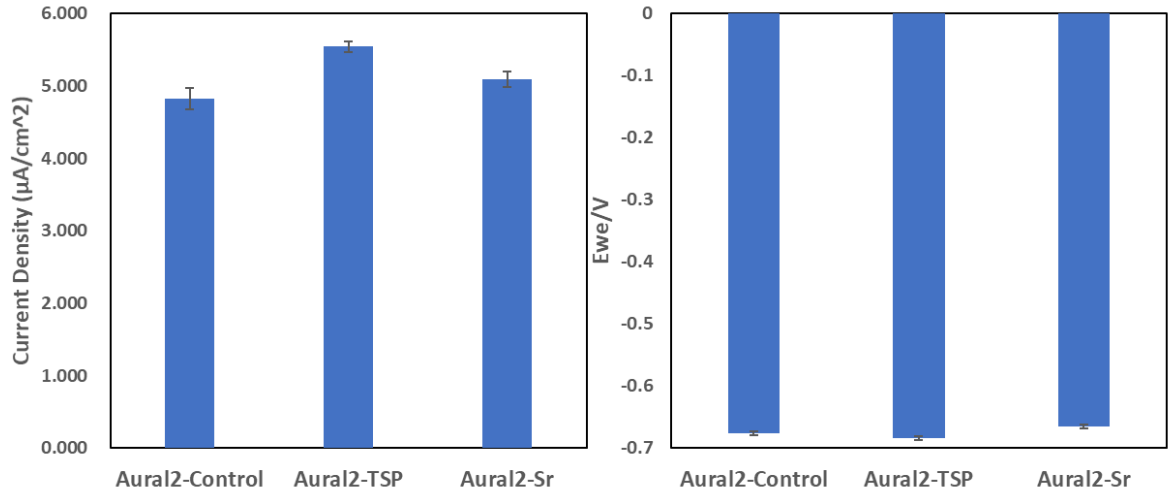


Figure 34. Corrosion current density and open circuit potential measurement of Aural2-Control, Aural2-TSP, and Aural2-Sr.

3.4 Conclusions

For all three alloys, the oxygen diffusion predominantly controlled the reduction reaction, therefore, the cathodic current density was not influenced by the applied potential significantly. The Al-7.5Si and W319 base alloy showed a lower anodic current density than Aural 2 alloy. Adding Sr or TSP to Al-7.5Si can refine the structure without increasing the corrosion rate. Even with different amount of TSP adding to the system, the corrosion rate was not affected significantly. W319 casting alloy has similar polarization behavior with Al-7.5Si alloy, but a decreasing in anodic current density with the microstructure modification was observed for Aural 2 alloy. This may due to the Aural 2 is near eutectic, but the other two are hypo-eutectic. Therefore, the microstructure of Aural 2 is expected to be refined to a higher degree than the other two alloys. The observation of the lower anodic current density as the surface is being anodically polarized is due to the Al oxide can passivate the surface and inhibit further corrosion, and the oxide is more compact and passive as the micro-galvanic cells become denser and finer. By comparing the polarization curves for Aural 2 alloy with Sr modification and with TSP modification, the results

show the microstructure refinement with Sr or TSP will not affect the corrosion behavior on the hypo-eutectic Al alloy, but will reduce the anodic current density of the eutectic Al alloy.

CHAPTER 4 SUMMARY AND FUTURE WORK

4.1 Summary

In this paper, we have carried out experiments to investigate the performance of TriSilanol POSS coating and modified alloys as well as the effect of microstructure on polarization behavior of Al-Si Based casting alloys. By the contact angle measurement, we successfully showed the increasing of the contact angle with the growth of the oxidation layer which follows the same trend with the literature by Dr. Swain's group. The contact angle of the uncoated 7075-T6 after exposure in the air for one day is around 38° and increases as the days increasing. [20] Their initial contact angle is larger than ours ($\sim 20^\circ$) due to the maximum exposure time for us is only 6 hours compared to theirs. For the powder form aluminum and copper, the performance of powder sedimentation changed due to the hydrophobicity changes with the coating of TSP. The maximal buoyant force for supporting powders floating on the water surfaces increases with the contact angle increases[21], which proves the hydrophobicity increases after coating with TSP. However, for aluminum powder is much more obvious is due to the much smaller density than the copper powder. Thus, the main sedimentation performance changes can be seen by the powder aggregation in the water. Furthermore, the contact angle measurement shows the dramatically increasing of the contact angle for TSP coated aluminum and copper plates, and the results for both Et-TSP and iBu-TSP samples are similar and have better hydrophobicity performance. We also proved that the physically wiping the surface would not affect the contact angles much, but re-soaking in pure ethanol solution will affect the durability of the TSP coating. However, we use copper powders to show the TSP coating will significantly delay the corrosion process when soaking in 3.5wt% NaCl solution. Later, the results for the modified Al-7.5Si samples showed that the TSP-modified and Sr-modified samples have smaller contact angles than unmodified samples, but the TSP-modified

and Sr-modified Aural 2 samples have larger contact angles than the unmodified ones. The contact angles measurement shows that the modification does not affect the hydrophobicity a lot, however, the contact angles for Sr-modified samples are always larger than the TSP-modified samples. By taking the SEM images of the unmodified, TSP-modified and Sr-modified Aural 2 samples, the slight changes in the surface wettability can be correlated to the topography differences of the samples. The results can be understood by either Wenzel's model [22] or Cassie-Baxter's model [23]. By the Wenzel's model, an increase in roughness will make a hydrophilic surface more hydrophilic, which can be seen that modified surface have finer microstructure compared to unmodified samples. By the Cassie-Baxter's model, the increase of the amplitude in roughness will increase the contact angles. The Sr-modified sample has the largest amplitude of roughness, which may cause additional air entrapment and contributes to the larger contact angles; and the unmodified sample has a smaller amplitude of roughness, which leads to smaller contact angles [24].

By the open circuit potential measurement, the results show that the unmodified Aural 2 has worst corrosion resistance among all three different materials, and unmodified W319 has the best corrosion resistance [9, 10]. The modification of three types of aluminum alloys only gives small changes for corrosion resistance. However, the TSP-modified samples are likely to have better corrosion resistance than the Sr-modified samples due to the higher open circuit potential for both Aural 2 and Al-7.5Si samples, while the different concentration of TSP will not affect the result much. The TSP-modified samples showed the better corrosion resistance than unmodified samples for all three types of aluminum alloys by comparing the E_{oc} of them, but Sr-modification only shows the beneficial in E_{oc} with Al-7.5Si, but not in Aural 2 alloys. By the potentiodynamic polarization measurement, the results showed the consistency with the open circuit potential

measurement. In the literature, the modified aluminum-silicon alloys tend to have a weaker corrosion resistance due to the increasing in boundaries between the Al-rich $[\alpha]$ phase and Si particles during growth from the melt [19], while the TSP modifier we used in this work makes the aluminum alloys have better corrosion resistance as well as a finer microstructure. Furthermore, in other literature, they mentioned that the finer dendritic structure tends to yield weaker corrosion resistance compared to the coarser dendritic structure [18]. To the contrast of their findings, our results indicate that the TSP-modified aluminum alloys have finer dendritic structure but also have better corrosion resistance. The polarization behaviors are similar between with Al-7.5Si alloy and W319, but a decreasing in anodic current density was observed for modified Aural 2 alloy. The microstructure of Aural 2 is expected to be refined to a higher degree than the other two alloys since it is near eutectic, while the other two are hypo-eutectic. At last, we can conclude that the corrosion behavior will not be affected for modification on hypo-eutectic Al alloy, but the anodic current density will be reduced for the eutectic Al alloys by comparing the polarization curves for modifications in all three types of materials.

4.2 Future Work

In addition to the experiment that we have done in this paper, there are several more improvements can be carried out to better support what we have concluded here. First, more SEM images can be taken for different samples with different modifications. Therefore, we can investigate the differences of the amplitude of the roughness for different samples and correlate the images with the contact angle measurements to prove the Wenzel's model or Cassie-Baxter's model for materials other than Aural 2 alloys. Second, we used 1wt% NaCl solution as the electrolyte in our polarization behavior, but in the real-world application, the concentration of 3.5wt% NaCl solutions may be a better approach. The effect of temperature and pH value for the

electrolyte can be tested to figure out the influence of the environment on the corrosion behavior of the aluminum alloys with and without modification. Third, the anodization process can be tested on the samples to see how the modified structure affect the process. The anodization process is an important application in the industry to create a fine layer of Al_2O_3 on the surface of the aluminum which helps with protection, decoration, insulation, wear-resisting and etc. The changing factor in structures and environment will affect the process of the anodization which may reduce or increase the cost for manufacturing. Therefore, the investigation of the anodization process on different types of aluminum alloys with and without modification is significant.

BIBLIOGRAPHY

BIBLIOGRAPHY

- [1] M. Tisza and I. Czinege, “Comparative study of the application of steels and aluminium in lightweight production of automotive parts,” *Int. J. Light. Mater. Manuf.*, vol. 1, no. 4, pp. 229–238, 2018.
- [2] Y. Lu, “A Novel Approach For Property Modification Of Cast Aluminum Alloys With Nanostructured Chemical Additions.” 2019.
- [3] R. Misra, A. H. Alidedeoglu, W. L. Jarrett, and S. E. Morgan, “Molecular miscibility and chain dynamics in POSS/polystyrene blends: Control of POSS preferential dispersion states,” *Polymer (Guildf)*., vol. 50, no. 13, pp. 2906–2918, 2009.
- [4] R. Misra, B. X. Fu, and S. E. Morgan, “Surface energetics, dispersion, and nanotribomechanical behavior of POSS/PP hybrid nanocomposites,” *J. Polym. Sci. Part B Polym. Phys.*, vol. 45, no. 17, pp. 2441–2455, Sep. 2007.
- [5] A. Fina, H. C. L. Abbenhuis, D. Tabuani, and G. Camino, “Metal functionalized POSS as fire retardants in polypropylene,” *Polym. Degrad. Stab.*, vol. 91, no. 10, pp. 2275–2281, 2006.
- [6] Y. C. Li, S. Mannen, J. Schulz, and J. C. Grunlan, “Growth and fire protection behavior of POSS-based multilayer thin films,” *J. Mater. Chem.*, vol. 21, no. 9, pp. 3060–3069, 2011.
- [7] D. Prządka, A. Marcinkowska, and E. Andrzejewska, “POSS-modified UV-curable coatings with improved scratch hardness and hydrophobicity,” *Prog. Org. Coatings*, vol. 100, pp. 165–172, 2016.
- [8] H. Ghanbari, B. G. Cousins, and A. M. Seifalian, “A nanocage for nanomedicine: Polyhedral oligomeric silsesquioxane (POSS),” *Macromol. Rapid Commun.*, vol. 32, no. 14, pp. 1032–1046, 2011.
- [9] K. Tanaka and Y. Chujo, “Advanced functional materials based on polyhedral oligomeric silsesquioxane (POSS),” *J. Mater. Chem.*, vol. 22, no. 5, pp. 1733–1746, 2012.
- [10] I. Jerman, A. Š. Vuk, M. Koželj, B. Orel, and J. Kovač, “A structural and corrosion study of triethoxysilyl functionalized POSS coatings on AA 2024 alloy,” *Langmuir*, vol. 24, no. 9, pp. 5029–5037, 2008.
- [11] Y. S. Lai, C. W. Tsai, H. W. Yang, G. P. Wang, and K. H. Wu, “Structural and electrochemical properties of polyurethanes/polyhedral oligomeric silsesquioxanes (PU/POSS) hybrid coatings on aluminum alloys,” *Mater. Chem. Phys.*, vol. 117, no. 1, pp. 91–98, 2009.

- [12] G. Markevicius *et al.*, “Polyoligomeric silsesquioxane (POSS)-hydrogenated polybutadiene polyurethane coatings for corrosion inhibition of AA2024,” *Prog. Org. Coatings*, vol. 75, no. 4, pp. 319–327, 2012.
- [13] P. Su *et al.*, “An evaluation of effects of molding compound properties on reliability of Cu wire components,” *Proc. - Electron. Components Technol. Conf.*, pp. 363–369, 2011.
- [14] Einar Bardal, *Corrosion and Protection*. 2004.
- [15] Y. Wu, “Corrosion-Induced Failure Analysis Of Cu Wire Bonded Packages,” 2018.
- [16] “ASTM G5-14 Standard Reference Test Method for Making Potentiodynamic Anodic Polarization Measurements,” West Conshohocken, 2014.
- [17] “The Measurement and Correction of Electrolyte Resistance in Electrochemical Tests,” *Meas. Correct. Electrolyte Resist. Electrochem. Tests*, 2009.
- [18] W. R. Osório, P. R. Goulart, and A. Garcia, “Effect of silicon content on microstructure and electrochemical behavior of hypoeutectic Al-Si alloys,” *Mater. Lett.*, vol. 62, no. 3, pp. 365–369, 2008.
- [19] W. R. Osório, N. Cheung, J. E. Spinelli, P. R. Goulart, and A. Garcia, “The effects of a eutectic modifier on microstructure and surface corrosion behavior of Al-Si hypoeutectic alloys,” *J. Solid State Electrochem.*, vol. 11, no. 10, pp. 1421–1427, 2007.
- [20] C. A. Munson and G. M. Swain, “Structure and chemical composition of different variants of a commercial trivalent chromium process (TCP) coating on aluminum alloy 7075-T6,” *Surf. Coatings Technol.*, vol. 315, pp. 150–162, 2017.
- [21] J. L. Liu, X. Q. Feng, and G. F. Wang, “Buoyant force and sinking conditions of a hydrophobic thin rod floating on water,” *Phys. Rev. E - Stat. Nonlinear, Soft Matter Phys.*, vol. 76, no. 6, pp. 1–9, 2007.
- [22] R. N. Wenzel, “Resistance of solid surfaces to wetting by water,” *Ind. Eng. Chem.*, vol. 28, no. 8, pp. 988–994, 1936.
- [23] A. B. D. Cassie and S. Baxter, “Wettability of Porous Surfaces,” *Trans. Faraday Soc.*, vol. 40, no. 5, pp. 546–551, 1944.
- [24] P. Bizi-Bandoki, S. Benayoun, S. Valette, B. Beaugiraud, and E. Audouard, “Modifications of roughness and wettability properties of metals induced by femtosecond laser treatment,” *Appl. Surf. Sci.*, vol. 257, no. 12, pp. 5213–5218, 2011.